Review

Novel Pharmaceutical Strategies for Enhancing Skin Penetration of Biomacromolecules

Luyu Zhang, Zirong Dong [ID], Wenjuan Liu, Xiying Wu, Haisheng He [ID], Yi Lu [ID], Wei Wu [ID] and Jianping Qi *[ID]

Key Laboratory of Smart Drug Delivery of MOE, School of Pharmacy, Fudan University, Shanghai 201203, China; 20211030023@fudan.edu.cn (L.Z.); 19211030076@fudan.edu.cn (Z.D.); 21111030046@fudan.edu.cn (W.L.); wxyifd@163.com (X.W.); he_haisheng@fudan.edu.cn (H.H.); fd_luyi@fudan.edu.cn (Y.L.); wuwei@shmu.edu.cn (W.W.)
* Correspondence: qijianping@fudan.edu.cn

Abstract: Skin delivery of biomacromolecules holds great advantages in the systemic and local treatment of multiple diseases. However, the densely packed stratum corneum and the tight junctions between keratinocytes stand as formidable skin barriers against the penetration of most drug molecules. The large molecular weight, high hydrophilicity, and lability nature of biomacromolecules pose further challenges to their skin penetration. Recently, novel penetration enhancers, nano vesicles, and microneedles have emerged as efficient strategies to deliver biomacromolecules deep into the skin to exert their therapeutic action. This paper reviews the potential application and mechanisms of novel skin delivery strategies with emphasis on the pharmaceutical formulations.

Keywords: skin delivery; macromolecules; ionic liquids; cell-penetrating peptides; nanoparticles; microneedles

1. Introduction

Transdermal delivery systems have undergone four decades of development since the first scopolamine transdermal patch was approved by the Food and Drug Administration (FDA) in the United States [1]. The skin delivery route constantly attracts academic and industrial attention for its unparallel advantages compared with oral delivery and hypodermic injection; these include the avoidance of drug degradation in the gastrointestinal tract and the hepatic first-pass effect; reduced fluctuation in plasma drug level; easy administration; good patient compliance; and immediate therapy termination via transdermal patch detachment in case of adverse side effects [2].

Meanwhile, macromolecular biologics, via the modalities of peptides, proteins, oligo-/poly-nucleotides, and polysaccharides, have taken up an increasing proportion of the available treatment over the years [3]. Biomacromolecules have high potential for transforming the current therapeutic regimen in treating skin diseases. For example, monoclonal antibodies of the immune checkpoints CTLA-4 (i.e., ipilimumab) and PD-1 (i.e., pembrolizumab and nivolumab) have been approved by the FDA for skin melanoma treatment as monotherapy, and trialed for combined therapy [4]. The gene silencing of tumor progression-related targets by siRNA may also serve a more durable purpose than the traditional small-molecule inhibitors. Other insightful research work has also shown the great potential of macromolecular biologics in treating chronic wounds [5–7], atopic dermatitis [8,9], psoriasis [10–12], etc.

Transcutaneous vaccination is rising, becoming a potent substitute for intramuscular inoculation to elicit a robust immune response with a lower antigen dose. The skin hosts abundant antigen-presenting cells in the dermis and viable epidermis, which, together with migratory T cells, contribute to the skin's immunocompetence and can be referred to as skin-associated lymphoid tissue (SALT) [13]. Preliminary research has shown that transcutaneous vaccination is quite effective against infectious pathogens such as hepatitis

B virus [14], *Streptococcus pneumoniae* [15], *Haemophilus influenzae* [16], and *Plasmodium falciparum* [17]. Additionally, antigen-encoded DNA, tumor-derived protein/peptide [18–21], and tumor cell lysate [22,23] have also been investigated as cutaneous vaccines for tumor immunotherapy, some of which have even entered clinical trials [24].

Nevertheless, poor skin permeability remains to be the primary downside of skin delivery. The compact structure of skin's outermost layer, namely the stratum corneum (SC), sets rather stringent requirements for transdermal drug candidates. The famous Lipinski's rule of five formerly proposed that poor drug-likeness for oral delivery is expected when the molecular weight (Mw) exceeds500, the number of hydrogen acceptors (NHAs) exceeds10, the number of hydrogen donors (NHDs) exceeds5, or the octanol–water partition coefficient (logP) exceeds5 [25]. This empirical rule can be extended to the skin delivery route [26]. Mw governs the partition coefficient, while logP reflects the SC–water partition. NHA and NHD indicate the interaction between drug molecules and the surfaces of corneocytes [27]. Accordingly, the physicochemical properties of biomacromolecules fail to meet the criteria for good drug-likeness in dermal or transdermal drug delivery. They are also extremely labile in their nature and prevalently necessitate parenteral delivery [28,29]. Therefore, an efficient penetration-enhancement strategy with low irritation and ease of use is the stepping stone to reach the full potential of dermal and transdermal biomacromolecule delivery. Currently, over 350 chemicals have been proposed as topical penetration enhancers, including surfactants, terpenes, sulfoxides, laurocapram, pyrrolidones, urea, fatty acids, etc. [30]. However, high potency often manifests with notable toxicity and skin irritation. Additionally, meddling with SC components could easily lead to skin dehydration and endogenous substance leakage [31]. Physical approaches using electrical, magnetic, photochemical, and ultrasonic waves have been investigated to enhance the skin penetration of therapeutics [32]. However, the cost and device portability of these physical approaches will eventually pose major hindrances during clinical uses. Therefore, physical approaches involving sophisticated devices will be intentionally left out in this review.

This review summarizes the recent development in enhancing the skin delivery of biomacromolecules, with highlights on rational formulation design and potential application. Novel penetration enhancers such as ionic liquids and cell-penetrating peptides as well as nano drug carriers will be elaborated. Even though a microneedle platform is more frequently assigned as a medical device or drug–device combination product, it is also included in this review to discuss the significance of microneedle formulation on drug-delivery behavior.

2. Physiological Barriers Hindering Skin Penetration of Biomacromolecules

The complex architecture of mammalian skin gives rise to its multi-faced functions, involving thermoregulation, sensation, metabolism, and immunization [33]. Most importantly, skin provides a bidirectional barrier against internal water or electrolyte loss as well as foreign insults [34]. Skin is generally comprised of three layers: the epidermis, dermis, and hypodermis (Figure 1a). The epidermis is outwardly composed of the *stratum basale* (SB), *stratum spinosum* (SS), *stratum granulosum* (SG), and *stratum corneum* (SC) [35], distinguished by the differentiation stages of keratinocytes (Figure 1b). Due to the existence of SC and tight junctions (TJs) [36–38], the epidermis has frequently been addressed as the rate-limiting mechanical barrier against the penetration of most drug molecules.

The SC is composed of 10–20 layers of non-viable cornified keratinocytes, which are more often termed as corneocytes [39]. Each corneocyte is encased in a hydrophobic cornified envelope that is tightly bound to the extracellular lipids, hindering the transdermal fluxes of hydrophilic substances [36,40]. SC lipids contain quasi-equimolar amounts of ceramides, free fatty acids, and cholesterol [41]. Ceramides found in the SC of human skin are considerably less polar than typical cell membrane lipids [42]. Generally, lamellar lipid layers in the SC exist in a densely packed orthorhombic phase (OR). The lipid chains in this phase adopt all-trans conformation and are packed in a rectangular crystalline lattice with no rotational or translational mobility [43]. Corneodesmosomes, the modified desmosomes

in the SC, further contribute to the reinforcement of corneocyte cohesion [44]. Together, the skin lipid lamellae, cornified envelopes, and corneocytes constitute the "brick and mortar" structure, which is the skin's first barrier against foreign insults as well as drug influxes [39].

TJs are found at the cell–cell borders in SG layers, which form a second barrier against the skin penetration of drug molecules by sealing the paracellular pathway. It is reported that TJ formation reduces the permeability of fluorescent tracer (332 Da) and dextran (40kDa) in a size-dependent manner [45]. TJs are dynamic protein complexes containing transmembrane proteins (e.g., claudins, occludins, and junctional adhesion molecules) as well as TJ plaque proteins (e.g., zonula occludens, and cingulin) [46] (Figure 1c). Claudins have been reported to be obligatory for the assembly of the TJ complex [47]. Mice with claudin-1 deficiency led to TJ barrier leakage to a ~600 Da tracer molecule [48].
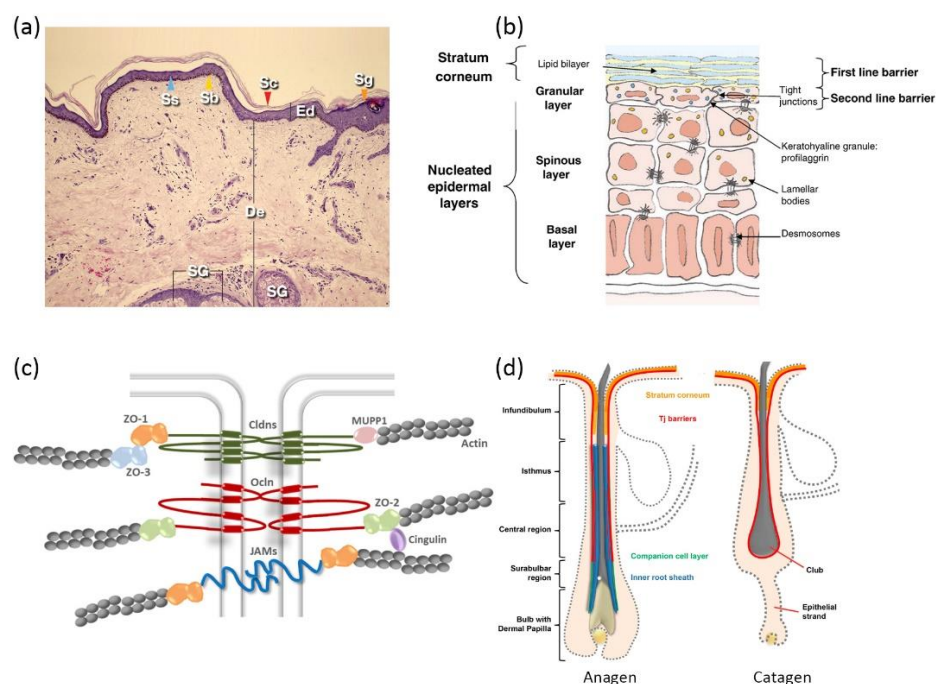

Figure 1. Schematic illustrations of skin: (**a**) histological cross-section of the skin (Ed—epidermis; Sc—stratum corneum; De—dermis; Sg—stratum granulosum; Ss—stratum spinosum; Sb—stratum basale; SG—sebaceous gland) (reproduced with permission from Arda et al., Clinics in Dermatology, adapted with permission from Ref. [49]. Copyright 2014 Elsevier); (**b**) epidermis structure (reproduced with permission from Baroni et al., Clinics in Dermatology; adapted with permission from Ref. [34]. Copyright 2012 Elsevier); (**c**) protein complexes of tight junctions (reproduced with permission from Basler et al., Journal of Controlled Release; adapted with permission from Ref. [46]. Copyright 2016 Elsevier); and (**d**) hair follicle structure of anagen phase and catagen phase (Reproduced with permission from Gorzelanny et al., Pharmaceutics; adapted with permission from Ref. [36]. Copyright 2020 MDPI).

Given the compact structure of epidermis, there exists three possible pathways for skin penetration, which can be designated as the paracellular pathway, transcellular pathway, and transappendageal pathway. The paracellular pathway is accomplished by diffusion into paracellular skin lipids, which is primarily favored by lipophilic small drug molecules. The transcellular pathway sets rigorous requirements for the physiochemical properties of drug molecules, since it involves consecutive partition and diffusion between hydrophilic and lipophilic domains [31]. Skin appendages take a rather limited role in the percutaneous penetration of most drug molecules, considering that they only take up a small proportion of the total skin area (<1%). However, various reports suggest that skin appendages (hair follicles in particular) appear to be an efficient penetration pathway and reservoir for

macromolecules [50–52]. Skin penetration via hair follicles (HFs) could seemingly bypass skin barriers such as the SC. However, a detailed investigation of HF anatomy unveiled that TJs are still present from the upper infundibulum down to the central region for HFs in anagen (i.e., the growing phase), and TJs completely cover the club hair in the catagen and telogen phases (i.e., the regression and resting phases) (Figure 1d). Additionally, SC is also found in the infundibulum, forming a double barrier in this region [53]. The dermal glands generally form TJ barriers, as well, but uptake via glands is not preferred due to their nature of inside-out secretion [54].

3. Novel Pharmaceutical Strategies for Skin Penetration

Efficient skin penetration is a prerequisite for biomacromolecules to exert their localized or systemic pharmacological actions. Considering biocompatibility, ease of use and the potential for massive production, this review summarizes novel penetration-enhancing strategies for biomacromolecules. We highlight the impact of pharmaceutical formulation design on skin-penetrating behavior. Ionic liquids and Cell penetrating peptides are proposed as novel penetration enhancers to deliver biologics deep into the skin via the disturbance of the SC layer and cell membrane [55,56]. Nanosystems of various materials and structures also pose as versatile vesicles to encapsulate biomacromolecules for enhancing penetration or increasing skin accumulation [57]. Microneedles could bypass the SC barrier and achieve instant or controlled drug release via fine-tuning of the matrix material [58]. A plethora of pilot investigations are incorporated in this review to discuss the drug-delivery performance and the potential application in disease treatment.

3.1. Ionic Liquids (ILs)

ILs are commonly defined as molten salts with melting points under 100 °C. Empirically, ILs are composed of bulky, asymmetric organic cations and weakly coordinating anions, hindering strong ionic interaction and disturbing the crystal lattice to retain liquid form at room temperature [59]. Principle synthesizing methods are feasible for scale-up production, including direct acid–base neutralization, salt metathesis in proper solution, and solvent-free metathesis via melting or grinding [60]. When ILs are not synthesized strictly according to stoichiometric ratio, excess neutral substances are also present in the systems. The definition of such systems sometimes overlaps with deep eutectic solvents (DESs). A DES is a mixture that exhibits lower melting points than any of its components. DESs and ILs are favored by different researchers with trivial differences: "ILs" emphasize ionic interaction while "DESs" highlight the profound hydrogen bonding [61]. For convenience, this review will uniformly address such systems as ILs.

IL-incorporated drug-delivery systems come with the merits of enhanced solubility and permeability for both polar and non-polar drugs [62]. The solvation ability is largely credited to anions' hydrogen bond forming and oxygen charge delocalization [60]. Erstwhile, research found that choline–geranate ILs (CAGE) could penetrate deep into the skin for deep-layer infection treatment with negligible toxicity to keratinocyte in mice [63]. Recent encouraging achievements were made by using ILs to enhance the skin penetration of biomacromolecules. Banerjee et al. firstly reported that CAGE could efficiently deliver bovine serum albumin (BSA, 66 kDa), ovalbumin (45 kDa), and insulin (5.8 kDa) deep into the epidermis and dermis of in vitro porcine skin in a time-dependent manner (Figure 2) [55]. However, the proportion of protein cargos in different skin layers may vary according to molecular weight. Compared to BSA, a larger portion of insulin was delivered into the epidermis, dermis, and receptor fluid after 24 h (80% for BSA and 93% for insulin). Protein-loaded ILs could further be integrated into biopolymeric film for improved mechanical strength [64]. CAGE could also facilitate the skin delivery of dextran with molecular weight up to 150k Da [65]. Choline-based ILs with other benign anions of different chain lengths and functional groups are also explored. Wu et al. reported that choline–malate IL could enhance the skin delivery of dextran two-fold [66], while choline–citric acid IL could enhance hyaluronic acid permeation five-fold [67]. Moreover,

the phosphate groups of siRNA could be directly taken as anions to form novel IL entities with proper cationic moieties for the dual purposes of enhanced skin transport and cell transfection [68].
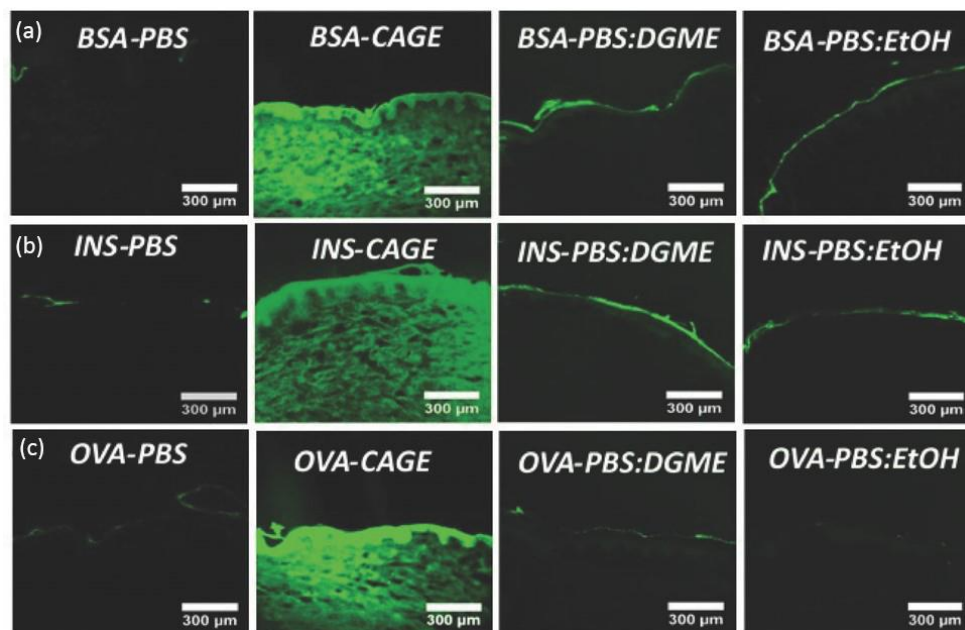

Figure 2. In vitro skin penetration of (**a**) FITC-BSA, (**b**) FITC-Insulin, and (**c**) FITC-OVA in PBS, CAGE, 50:50 (*v/v*) PBS/DGME, and 50:50 (*v/v*) PBS/ethanol, respectively. BSA—bovine serum albumin; INS—insulin; OVA—ovalbumin; PBS—phosphate buffered saline; DGME—diethylene glycol monoethyl ether (reproduced with permission from Banerjee et al., Advanced Healthcare Materials; adapted with permission from Ref. [55]. Copyright 2017 Wiley).

Given the amphiphilic nature, ILs based on choline–fatty acids were scrutinized as surface active reagents to incorporate hydrophilic biomacromolecules into a classic oil-based penetration enhancer such as isopropyl myristate (IPM) [69–71]. Tahara et al. recently reported that ILs derived from choline and oleic acid ([Ch][Ole]) facilitated the dispersion of antigenic peptides in IPM and ethanol (EtOH). The formulation showed little skin irritation, and the transdermal flux of peptide in IL/IPM/EtOH was 28- and 9-times higher than that in EtOH/PBS and EtOH/IPM, respectively [69]. The EtOH phase could be substituted with another hydrophilic IL derived from choline and propionic acid to robe the biologics before mixing with [Ch][Ole] and IPM [71]. A similar strategy was explored to disperse insulin in IPM for transdermal delivery, with [Ch][Ole] as a surfactant and Span-20 as a co-surfactant [70]. The IL-assisted microemulsion enabled higher bioavailability in systemic circulation and sustained insulin levels for a longer period (half-life > 24 h) compared to subcutaneous injection [70].

The latest work in this field pays extra attention to biomacromolecule stability during the formulation and drug delivering process. Tailor-made ILs with self-buffering capability could offer additional protection for macromolecules' thermal, structural, and biological stability [72]. For example, the addition of a buffered choline–dihydrogen phosphate IL could substantially prolong the shelf-life of siRNA up to three months [73]. As another example, molecular simulation results indicated that CAGE could stabilize insulin by occupying the solvation shell of insulin, concomitantly exiling water molecules from the insulin surface [74]. Furthermore, an IL mixture of CAGE and choline–phenylpropanoic acid (CAPA) was designed to topically deliver siRNA for psoriasis treatment [10]. CAGE played the role of permeation enhancer, while CAPA retained the secondary structure of siRNA, probably owing to the intercalation between RNA base pairs and CAPA's aromatic rings [10].

The mechanism behind ILs' permeation enhancement is still in debate. Rudimentary theory involves SC lipid extraction by ILs [55,75]. ILs also enable SC lipids to transform from the orthorhombic phase to liquid crystalline packing, resulting in greater lipid fluidity [76]. In addition, an increase in unordered protein in SC was observed, while the deeper epidermis was not significantly affected [65]. Morphological examination found distinct gaps among lipid lamella, and the "brick and mortar" structure of SC became less densely packed after IL treatment [77]. The anion/cation ratio of ILs governs hydrogen bonding and ion pairing, which directly influences the viscosity, conductivity, and diffusivity of the IL formulation. Profound proton exchange also exists between the ions and the excess neutral components. Tanner et al. investigated the significance of ion ratio for CAGE's penetration ability in the context of insulin delivery [75]. CAGE with an ion ratio of 1:1 exhibited the highest degree of ion pairing but the lowest permeation enhancement, presumably owing to the ions' preference to interact with each other rather than with macromolecular drug or skin lipids. Moreover, the internal structure of ILs may alter when exposed to body fluid or water dilution. Taking CAGE as an example, a 25–50 vol% of water would transfer ILs into the lamellar phase, while further dilution would lead to micelle formation via aggregation of geranate anions' hydrophobic chains [78]. However, current research works seldom discuss the influence of hydration state on the permeation enhancement of ILs.

3.2. Cell-Penetrating Peptides (CPPs)

CPPs comprise a family of short peptides (5–30 amino acids) that have demonstrated impressive penetration across bio-barriers without damaging the membrane integrity [79]. Commonly used CPPs bear positive charges owing to arginine and lysine residues (such as TAT, DPV3, and R8). Around 44% of CPPs are amphiphilic, characterized by a proline-enriched sequence or a combination of hydrophobic and polar regions in either the first or secondary structure (such as BPrPr, pVEC, and ARF). Hydrophobic CPPs (such as K-FGF, C105Y, gH625) only take up 15% of the whole CPP family [80].

A naturally derived protein bank contains rich resources for CPP design, such as heparin-binding proteins, signal peptides, nucleic acid-binding proteins, and anti-microbial peptides [81]. Certain CPPs could, additionally, serve as ligands for target delivery, bringing extra benefits for treating malignant skin diseases such as melanoma [82]. However, extracting CPPs from their original proteins may alter their secondary conformation and result in a loss of penetration ability. Artificially designed CPPs have further diversified the CPP bank by introducing novel sequences, unnatural amino acids [83] or even modified shapes such as dendrimers [84] and cyclic rings [85]. These exquisitely designed CPPs substantially improve the cargo-loading efficiency as well as resistance against cellular degradation. Additionally, carbohydrate scaffolds modified with guanidine could substitute the typical peptide backbone as transdermal enhancers. For example, a sorbitol-based carrier with 8 units of guanidine (Sor-G8) was shown to be more efficient than the arginine-rich CPP, R8, regarding skin-penetration ability [86].

The inchoate formulation strategy adopts a simple physical complexation of CPPs and biomacromolecules via electrostatic or hydrophobic interaction. An excessive CPP ratio is preferred to form positively charged nano-scale complexes. Chen et al. identified a cyclic CPP named TD-1(ACSSSPSKHCG) via phage display, which facilitated the transdermal delivery of insulin via simple coadministration and suppressed blood glucose levels for at least 11 h [87]. However, physical complexation via bulk mixing unavoidably results in poly-dispersed particle size or heterogeneous nanostructures, which potentially hinder transdermal efficacy. As for chemical conjugation, proteins and oligonucleotides are compatible for direct CPP conjugation via amino/sulfide bonds or PEG linkage. However, the multiple active sites on the cargos may result in uncontrollable conjugation.

Recombinant protein is a rather advanced strategy to achieve site-specific and homogeneous CPP conjugation [88]. For instance, TD-1 could be incorporated to construct a fusion protein with human epidermal growth factor (hEGF) without deactivating the latter. The resulting fusion protein TD-1-hEGF exhibited higher skin-penetration ability than the

simple co-administration of TD-1 and hEGF [79]. In another case, Gautam et al. utilized a novel human-derived arginine-rich CPP, IMT-P8, to construct a fusion protein with green fluorescence protein (GFP) and proapoptotic peptide KLA. A large amount of IMT-P8-GFP and IMT-P8-KLA was detected in viable epidermis and hair follicles, and the delivery efficiency of IMT-P8 was even higher than the classical TAT [89]. Another approach is to construct a CPP fusion protein with a ligand to enhance target delivery within the skin. Considering that epidermal growth factor (EGF) is overexpressed in many tumor cells, a fusion protein of EGF (ligand) and SPACE (CPP) was constructed to deliver antineoplastic siRNA [90]. Moreover, it is a common strategy to attach CPPs to nanovesicles for enhanced skin delivery, which will be discussed in the next section.

The specific mechanisms of CPP–cargo translocation are contingent on several factors, including the nature of cargos (type, size, and charge), the physicochemical properties of CPPs (molecular weight, charge delocalization, and hydrophobicity), and even the experimental condition (pH, temperature, CPP concentration, and cell line types). Generally, cellular uptake is initiated by cellular contact between the cationic CPP and anionic phospholipid bilayers, glycosaminoglycans, or proteoglycans on the cell surface [56]. Thereafter, the internalization of CPP-cargo complexes can be divided into an energy-independent pathway (i.e., direct translocation) and an energy-dependent pathway (i.e., endocytosis) (Figure 3). Three models of energy-independent translocation were proposed: (1) the inverted micelle model [91]; (2) the carpet-like model [92]; and (3) the transient-pore model [93]. As for the active penetration pathway, endocytosis can be further divided into phagocytosis and pinocytosis (including macropinocytosis, clathrin-mediated endocytosis, caveolae-mediated endocytosis, and clathrin- and caveolae-independent endocytosis). The detailed mechanism of CPP-cargo internalization is beyond the scope of this review, but can be read about in the newly published literature [56,80,81,94,95].
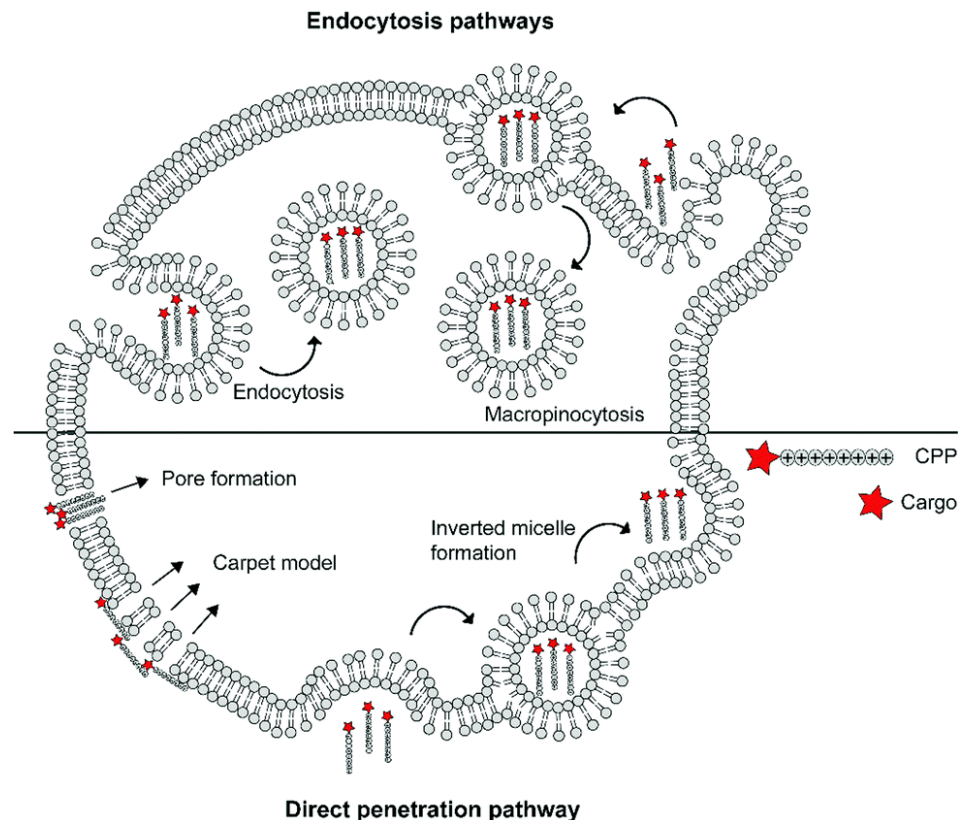

Figure 3. Schematic summary of different mechanisms underlying the cellular uptake of cell-penetrating peptide (reproduced with permission from de Jong et al., RSC Chemical Biology; published by RSC Publishing, 2020) [96].

3.3. Nanotechnology

Nanotechnology is trending in all aspects of drug delivery for increased efficacy and decreased toxicity, drawing attention to its unique nano-size effect as well as its versatility in surface modification. Having gone through several decades of development, nano-scale drug-delivery vesicles (<500 nm) now adopt different forms including nanoparticles, nanotubes, nanoemulsions, liposomes, micelles, etc. Endowed by their physio-chemical properties and surface modification, nanovesicles serve multiple purposes of enhanced drug solubility and permeability, target enrichment, bio-response to their microenvironment, and evasion from immune elimination. Nano-encapsulation also provides effective protection for liable biologic therapeutics against ambient degradation factors. Therefore, various nanovesicles have been reported to load biomacromolecules for enhanced skin penetration and increased skin accumulation (Table 1).

Table 1. Current reports of using nanovesicles for dermal and transdermal delivery of biomacro-molecules.

Nanocarrier	Composition	Particle Size/ζ-Potential	Cargo	Indication	Ref.
Gold nanoparticle	AuNPs in Pluronic F-127 gel	190~208 nm/ +30~ +45 mV	PGT DsiRNA	Diabetic wound-healing	[97]
	AuNPs with PEI and TAT conjugation	199 $\pm$ 7.76 nm/ 16.81 $\pm$ 0.56 mV	pDNAs encoding microRNA-221 inhibitor gene	Melanoma	[98]
	AuNPs modified with thiolated siRNA and PEG coating	12.38 $\pm$ 1.59 nm/~28 mV before coating	EGFR siRNA	Psoriasis	[99]
	AuNPs modified with thiolated siRNA and thiolated oligoethylene glycol	28 $\pm$ 3 nm/-	GM3S siRNA	Diabetic wound-healing	[100]
	AuNPs with PEI and LL37 coating	7.6 $\pm$ 0.9 nm/ 36.8 $\pm$ 2.3mV	pDNA encoding VEGF	Diabetic wound-healing	[101]
	AuNP-CONH-VEGF	11.2nm $\pm$ 0.1 nm/-	VEGF	Wound healing	[102]
	AuNP-CONH-KGF	65.7 nm/$-$ 34.9 mV	KGF	Wound healing	[103]
	AuNPs	11.6 nm/18.3 mV	HRP, β-gal, OVA	-	[104]
	AuNP-PEG- Esc(1-21)	~14 nm/$-$35.58 mV	Antimicrobial peptide Esc(1-21)	Antipseudomonal wound healing	[105]
Carbon nanotube	PEI functionalized carbon nanotubes	-/40~60 mV	BRAF siRNA	Melanoma	[106]
Mesoporous silica nanoparticle	Mesoporous silica nanoparticles with poly-L-lysine coating	200 nm/$-$34 mV	TGFβR-1 siRNA	Facile skin cancer	[107]
Nanostructured lipid carrier	0.5% glycerol distearate, 0.25% oleic acid, 0.25% PEI, 1.0% Poloxamer 407, and pH7.4 phosphate buffer	230 nm/+10 mV	TNFα siRNA	Psoriasis	[108]
	DOTAP/sodium cholate/coiled-coil protein = 60:10:7	174.22 $\pm$ 8.71 nm/ 34.5 $\pm$ 1.7 mV	Keap1 siRNA	Diabetic wound-healing	[109]
	Elastic liposomes. DOTAP/DOPE/Cholesterol = 6:4.2:1.8(w/w/w)	147.7 $\pm$ 31.9 nm/ 46.7 $\pm$ 13.4 mV	antagomiR-203 or SOCS3 siRNA	Psoriasis	[110]
	Elastic liposomes. Soya phosphatidylcholine/span 80 = 86:14 (w/w)	122 $\pm$ 9.2 nm/-	P. falciparum surface antigen, MSP-1$_{19}$	Malaria vaccine	[17]
	Elastic liposomes. Soya phosphatidylcholine/span 80 = 86:14 (w/w)	123.8 $\pm$ 51.31 nm/ 9.36 mV	Recombinant fusion protein PfMSP-Fu$_{24}$	Malaria vaccine	[111]
	Elastic liposomes. HPC/cholesterol/DOTAP = 8:4:1 (molar ratio)	107 $\pm$ 0.757nm/ 56.5 $\pm$ 1.13mV	Growth factors fused with low-molecular-weight protamine	Diabetic wound-healing	[5]
	SECosomes. DOTAP/DOPE/NaChol = 6:1:1(w/w/w), rehydrated in 30% ethanol	172 nm/44 mV	DEFB4 siRNA	Psoriasis	[112]
	Deformable cationic liposomes. Octadecylamine/cholesterol = 10:1	208.5 $\pm$ 11.5 nm/-	pDNA encoding HBsAg	Hepatitis B vaccination	[113]
	Niosomes. Span85/cholesterol = 7:3	2.3 $\pm$ 0.15 μm/-	pDNA encoding HBsAg	Hepatitis B vaccination	[114]

Table 1. *Cont.*

Nanocarrier	Composition	Particle Size/ζ-Potential	Cargo	Indication	Ref.
	Ethosomes. DOTAP/cholesterol = 5:1, with SPACE modification	108.4 ± 3.4nm/ 49.1 ± 0.6mV	GAPDH-siRNA-SPACE conjugate	-	[115]
	Pyrrolidinium lipid/1,2-di-(9Z-octadecenoyl)-snglycero-3-phosphocholine/DOPE/DSPE-PEG2000 = 1:2:2:0.2	102 ± 6 nm/ 32.14 ± 6.21 mV	STAT3 siRNA and TNFα siRNA	Psoriasis	[116]
	Lipidoid 306O$_{13}$/DSPC/cholesterol/C14-PEG = 50:10:38.5:1.5ao	110 nm/-	TNFα siRNA	Diabetic wound-healing	[117]
	DOPC and cholesterol-conjugated oligonucleotides	21 ± 2 nm	IL17RA gapmer antisense oligonucleotide	Psoriasis	[11]
	Poloxamer 188/Tween 80/Precirol® ATO 5/Miglyol® 812 N (1:2:10:1)	273.6 ± 27.64 nm/ ~31.63 ± 1.9 mV	Antimicrobial peptide LL37	Wound healing	[118]
	Lipidic blend containing Precirol® ATO 5/Miglyol® 182 (10:1), emulsified with 0.67% (w/v) Poloxamer and 1.33% (w/v) polysorbate 80	335 nm/-27 mV	Recombinant human epidermal growth factor	Wound healing	[119]
Hybrid lipid–polymer nanoparticle	Inner PLGA core coated with cyclic head lipid/DOPC/DSPE-PEG2000(4.0/4.5/1.5, molar ratio)	163 ± 9 nm/ 35.14 ± 8.23 mV	TNFα siRNA	Skin inflammation	[120]
	2.0% of Compritol® 888 ATO (lipid), 1.5% of poloxamer 188 and 0.1% of the cationic polymer poly(allylamine hydrochloride)	142 nm/+25 mV	TNFα siRNA	Psoriasis	[121]
Liquid crystalline nanodispersion	MO:OA:PEI:Aqueous phase(Tris-HCl) = 8:2:1:89 or 8:1:0.5:90.5 (w/w/w/w)	220 nm/1 mV or 170 nm/− 2 mV	TyRP-1 siRNA	Vitiligo	[122]
	MO/OA/PEI/aqueous phase 8/2/1/89 w/w/w/w, functionalized with TAT	310 ± 8 nm/ 1.19 ± 0.27 mV	TNFα siRNA	Inflammation	[123]
	MO/OA/poloxamer/aqueous phase 8:2:0.9:89.1 w/w/w/w	181.77 ± 1.08 nm/-	Cyclosporin A	-	[124]
	MO/OA/PEI/aqueous phase 8/2/1/89 w/w/w/w	215.4 ± 7.9 nm/ 0.7 ± 1.0 mV	IL-6 siRNA	Psoriasis	[125]
	Poloxamer 407 containing 0.5% liquid crystalline gel (glycerol monooleate/water 70:30)	~130 nm/+3~ +11 mV	Antimicrobial peptide LL37	Wound healing	[126]
Dendrimer	TAT-conjugated PAMAM	106 nm/+45 mV	pDNA encoding GFP	DNA vaccine	[127]
Non-ionic colloidal carrier system	DMSO/IPM/Tween 80/Span 20 (0.45/2.5/0.3/0.2, v/v/v/v)	100.6 ± 28.3 nm/-	Insulin	Diabetes	[128]
SAMiRNA (self-assembled micelle)	PEG and hydrocarbon conjugation at each end of unmodified oligonucleotides	<100 nm/neutral	Dual-conjugated DNA/RNA heteroduplex	Androgenetic alopecia	[129]
Polysaccharide nanoparticles	Panax quinquefolium polysaccharide	20 nm/-	Panax quinquefolium polysaccharide	UVB-induced skin cancer	[130]
Ginsenoside nanoparticles	Ginsenosides/insulin (25:1, w/w) self-assembly	165.5 ± 0.6 nm/-	Insulin	Diabetes	[131]

3.3.1. Inorganic Nanoparticles

Inorganic nanoparticles in the forms of metallic nanoparticles, mesoporous silica nanoparticles, quantum dots, and carbon tubes have been proposed as transdermal vesicles. Gold nanoparticles (AuNPs) are rigid metallic nanoparticles that often come with a small size (<30 nm) and high compatibility. Surface modification can easily be achieved via Au-S interaction. AuNPs have been shown to disrupt phospholipid layers and modulate lipid-phase transitions, transiently increasing skin porosity and lipid fluidity [132]. Chen et al. attached vascular endothelial growth factor (VEGF) to AuNPs via a pegylated linker. Even with negative surface charge, such vesicles of approximately 20nm were able to deliver VEGF to the subcutaneous region and promoted subcutaneous angiogenesis 7 days after the topical treatment [102]. Huang et al. investigated the potential transcutaneous

immunization effect via simple co-administration of ovalbumin and superfine AuNPs (<10 nm) [104]. The macromolecules were mainly detected in the epidermis with no biased accumulation in hair follicles, slowly migrating to the deeper layers. The topical treatment elicited robust and consistent immunization, with anti-OVA IgG levels comparable to intramuscular inoculation [104]. AuNPs could be functionalized with CPPs to improve the transfection of gene materials. For instance, Niu et al. loaded TAT-conjugated AuNPs with miRNA-221-encoded plasmid DNA for melanoma treatment. A skin-penetration test found large amounts of AuNPs in hair follicles, with detectable traces deep into the dermis at ~80 μm. In vivo experiments on tumor-bearing mice showed attenuated tumor growth and apoptosis of tumor cells [98].

Other modalities of inorganic nanoparticles have also been reported for skin delivery. Lio et al. chose mesoporous silica nanoparticles (MSNs) to load siRNA for facile skin cancer treatment [107]. Siu et al. utilized polyetherimide (PEI)-functionalized single-walled carbon nanotubes as siRNA carriers to treat melanoma. They proposed that carbon nanotubes could act as "nano needles" and penetrate cells via a diffusion-like mechanism. In vivo gene silencing as well as tumor inhibition were demonstrated on CD-1 mice [106]. PEI could also be conjugated to lipopolymers such as DSPE-PEG before being non-covalently attached to carbon nanotubes, suggesting a simpler and more expeditious preparation method [133].

3.3.2. Lipid-Based Nanocarriers

Liposomal formulation is among the most-studied lipid-based nanocarriers. Liposomes are generally spherical vesicles containing single or multiple phospholipid bilayers and an aqueous core. Conventional liposomes tend to be rigid and unyielding, rendering it hard for them to penetrate the SC as whole [134]. The encapsulated therapeutics are mostly deposited in superficial skin layers, being released via the exchange of the lipid component between liposomes and the SC. To reach a therapeutic concentration at deeper skin layers, Cevc et al. proposed ultra-deformable lipid vesicles called transfersomes [135]. Transfersomes have been reported to be effective for the transdermal delivery of insulin, inducing hypoglycemia in healthy human volunteers [135]. With polysorbate or sodium cholate as edge activators, transfersomes are expected to squeeze through the paracellular pathways in the SC. In addition to the role of edge activator, sodium cholate could create pores in the SC during its protonation, hence, delivering macromolecular cargo into deeper skin layers [136].

The promising results of transfersomes stimulated the development of novel elastic liposomes. They are endowed with deformability via the incorporation of surfactants to lower the phase-transition temperature of lipid vesicles. These elastic liposomes can be further categorized as niosomes, ethosomes, invasomes, SECosomes, and PEVs. Invasomes are composed of soy phosphatidylcholine, lysophosphatidylcholine, terpenes, and ethanol [137]. As traditional penetration enhancer, ethanol could interact with the polar regions of SC lipids, increasing the lipid fluidity of both the SC and vesicles [138]. Terpenes could also increase lipid fluidity and enhance drug diffusion into the intercellular lipids of SC [137]. Niosomes are self-assembled vesicles, characterized by non-ionic surfactants and cholesterol. Masheswari et al. reported a successful case of using niosomes to encapsulate Hepatitis B surface protein as an antigen and cholera toxin B as an adjuvant for transcutaneous immunization [14]. Even though the particle size of encapsulated niosomes reaches 2.83 ± 0.29 μm, more than half of the loaded antigens were deposited in the deeper SC layers and epidermis, eliciting strong immune response compared to intramuscular inoculation. Ethosomes contain a significant amount of ethanol (20–50%) [139]. Chen et al. designed a cationic ethosomal vesicle for the skin delivery of CPP-conjugated siRNA and achieved $63.2\% \pm 7.7\%$ target-gene knockdown in mice [115]. The definition and classification of the above elastic liposomal vesicles can slightly vary among different reviews and research articles. Hence, the formulation and vesicle characterization should be given specific attention when cross-evaluating different literature.

3.3.3. Lyotropic Liquid Crystalline Nanodispersions (LLCs)

LLCs are characterized by an ordered internal structure and large interfacial area, serving the purposes of enhanced drug solubility, modulated drug release, and minimized side effects. Lopes et al. firstly reported the reverse hexagonal phase nanodispersion of monoolein (MO) and oleic acid (OA) for the topical delivery of a model peptide, cyclosporin A [124]. Later, several studies introduced PEI into liquid crystals to bind and condense nucleic acids for efficient cutaneous gene delivery. LLC containing MO/OA/PEI formed a disordered hexagonal structure, while the incorporation of siRNA had no effect on the liquid crystalline nanostructure [140]. Depieri et al. further optimized the system by reducing the PEI concentration, and they successfully used it to deliver interleukin-6 siRNA in a psoriasis skin model [125]. Furthermore, Petrilli et al. complexed siRNA with CPPs before adding to MO/OA/PEI LLC. Topical application on a skin inflammation animal model confirmed that the combination of CPPs and nanodispersion brought even higher gene-silencing efficacy than LLCs alone [123].

3.3.4. Dendrimers

Dendrimers embody a central atom core and outwardly branched structure with a large cavity between the branches to incorporate therapeutic molecules. The internal structure and particle size are determined by different preparation methods as well as synthesis generations (G0-10). The surface charge can also be modulated by amine, carboxyl, acetyl, and hydroxyl group modification on the branches [141]. Moreover, CPP conjugation can further enhance permeability. Polyamidoamine (PAMAM) is the most-investigated material for dendrimers. TAT-conjugated PAMAM dendrimers have been reported to load plasmid DNA for transcutaneous vaccination [127,142]. The compact structure of dendrimers ensured protection against DNA degradation. The possible mechanism of skin penetration for dendrimers can be elucidated as follows: (1) dendrimers serve as drug reservoir to boost drug flux into the skin; (2) when dendrimers are composed of penetration-enhancing materials (e.g., IPM), they can perturb the skin via liquefaction or dissolution of SC lipids; and (3) with proper surface modification, dendrimers are prone to accumulating in hair follicles in a time-dependent manner [143].

3.4. Microneedles (MNs)

MNs have been emerging as a promising solution for transdermal drug delivery since the 1990s [144]. An MN patch contains an array of micro-scale needles (length < 1000 µm), which can directly pierce through the SC and create transient microchannels for the delivery of various drugs without introducing physical pain [145]. Theoretically, MN platforms cast no limitation over drug molecular weight and hydrophilicity. Therefore, hydrophilic biomacromolecules such as proteins and nucleic acids can be encapsulated into MNs for vaccination as well as the treatment of melanoma, diabetes, and beyond [58,146]. Inorganic materials such as silicon, stainless steel, glass, and ceramics were firstly used to fabricate solid MNs. However, they still pose disadvantages such as insufficient drug payload, a complicated fabrication process, and biohazardous needle sharps. In the past decade, polymers have been highlighted as promising materials for new generations of MNs due to their excellent biocompatibility, versatility, and cost-effectiveness [147]. Polymeric MN insertion ability is governed by the MN fabrication method and MN array geometry (aspect ratio, needle density, base thickness, tip angle, etc.), which are also associated with the pain level perceived by patients [148]. Drug-release rate can also be tuned by adjusting the polymeric material composition.

3.4.1. Dissolvable MNs

Upon insertion, dissolvable MNs are able to quickly dissolve into the skin, which is favorable for instant drug release [149]. Polysaccharides such as dextran, sodium chondroitin sulfate, hydroxypropyl cellulose (HPC), carboxymethyl cellulose (CMC), hydroxypropyl methylcellulose (HPMC), sodium alginate, and hyaluronic acid (HA) contain abundant

hydrophilic groups, making them desired substrate polymers for dissolvable MNs [145]. Dissolvable MNs based on chondroitin sulfate and dextran were reported to deliver recombinant human growth hormone in the form of solid dispersion, reaching peak plasma concentration in 15 min after topical application [150]. The addition of lightly cross-linked polymers as well as materials with larger molecular weight could compensate for insufficient mechanical strength. For example, Chen et al. prepared two-layer dissolvable patches from gelatin and sodium CMC for insulin delivery [151]. These patches exhibited sufficient insertion into mouse cadaveric skin under an application force of 9 N, followed by complete dissolution after 1 h [151]. In another case, insulin delivered via starch/gelatin dissolvable MNs were able to attain relative bioavailability of 92% [152]. The shelf-life of insulin in such MNs was reported to be 20–30 days [152,153]. Additionally, the incorporation of low-dose graphene oxide could endow dissolvable MNs with beneficial properties such as enhanced mechanic strength, moisture resistance, and anti-bacterial and anti-inflammatory effects [154].

Dissolvable MNs are compatible to load nanoparticles for more intricate therapeutic purposes. Lopez-Ramirez et al. reported a magnesium (Mg)-microparticle-embedded dissolvable MN patch to actively deliver anti-CTLA-4 antibodies in a melanoma mouse model [155]. In contact with interstitial biofluid, Mg microparticles could instantly generate hydrogen bubbles, which induced significant vortex flow fields at localized sites and served as a "pumping-like" force for deeper and faster dermal delivery [155]. Furthermore, the addition of cowpea mosaic virus nanoparticles into the MNs could vigorously activate the innate immune system and shift the immunosuppressive tumor microenvironment into an immunostimulatory state [156]. As another example, Zeng et al. utilized an MN platform to deliver glucose oxidase (GOx) for tumor starvation therapy. The coated GOx was loaded into dissolvable MNs and demonstrated a catalysis duration of at least 6 days under biological conditions [157].

3.4.2. Biodegradable Polymeric MNs

Biodegradable polymer-based MNs are used to achieve sustained drug release up to months for drugs such as insulin and contraceptives, obviating the inconvenience of frequent administration [158]. Natural biodegradable polymers such as chitosan [159], silk [160], and chitin [161] are considered ideal candidate materials. Wang et al. fabricated insulin-loaded silk fibroin MNs with a sustained insulin release of up to 60 h [160]. However, these patches need to remain adherent to the skin for days to achieve long-period degradation. To address this inconvenience, a combined patch of antigen-loaded degradable MN tips and a dissolvable supporting matrix was reported by Chen et al. [162]. The supporting array was composed of PVP/PVA and quickly dissolved upon insertion, implanting chitosan MN tips in the dermal layer. A sustained release of up to 28 days was achieved in mice [162]. Synthetic degradable polymers including polylactic acid (PLA), polyglycolic acid (PGA), poly(lactic-co-glycolic acid) (PLGA), polycarbonate, polystyrene (PS), and polycaprolactone (PCL) [145] have also been exploited. For further MN modification, one could consider the encapsulation of functional particles such as magnetic graphene quantum dots [163], reduced graphene oxide nanocomposites [164], and graphene quantum dots [165], which render MNs compatible for electroporation or iontophoresis. Biodegradable polymers mostly share the common properties of dissolving in organic solvents or melting at high temperatures. Hence, the fabrication usually involves organic solvents or high temperature to form MNs in micromolds. Sensitive drugs such as peptides, proteins, and nucleic acids are susceptible to such process. Thus, facile fabrication methods such as electro-drawing are to be further developed [166].

3.4.3. Swellable Polymeric MNs

Swellable polymeric MNs are able to absorb large quantities of water in the presence of interstitial fluid and remain insoluble due to the strong chemical or physical chain crosslinking within the polymer matrix. On swelling, they serve as a release-rate-controlling

membrane, which can be tuned by modulating the crosslinking density [167]. Polymers that meet the criteria for swellable MN fabrication include poly(hydroxyethylmethacrylate) (PHEMA), acrylate-modified HA (m-HA), polystyrene-block-poly (acrylic acid) (PS-b-PAA), and poly (methyl vinyl ether-co-maleic acid) (PMVE/MA) [168]. Donnelly et al. reported the preparation of PMVE/MA-based MNs, crosslinked with PEG via esterification [169]. PMVE/MA-PEG swelled 3-fold and 50-fold after cross-linking for 24 h and 72 h, respectively. However, cross-linking for the above polymers usually requires high temperature (e.g., 80 °C for PMVE/MA-PEG crosslinking [169]). It is advised that sensitive drugs be post-loaded into the backing adhesive patches as drug reservoirs after the cross-linking process. A mild fabrication method was reported by Yin et al. using 2-ethoxyethanol to endow silk fibroin with swellable and insoluble properties at 25 °C [170]. By increasing the 2-ethoxyethanol/silk fibroin blending ratio, larger swelling capacities up to 800% were shown after insertion, accompanied by porous network formation to facilitate macromolecular drug release [170].

3.4.4. Bio-Responsive MNs

The unique physiological disease microenvironment is utilized to trigger drug release from bio-responsive MNs, including pH, glucose, hypoxia, temperature, enzymes, and receptors [147]. Glucose-responsive insulin delivery is the most-discussed solution for regulating blood glucose without inducing hypoglycemia [171]. Bio-responsive MN is a versatile platform to mimic pancreatic endocrine function either by incorporating glucose-sensitive matrix material or by encapsulating stimuli-responsive nanoparticles to adjust insulin release according to endogenous glucose level. For the former strategy, cationic polymers modified with phenylboronic acid were reported to release insulin via a glucose-triggered charge switch [172,173]. MNs were prepared via in situ photopolymerization of the insulin and matrix monomer premixture, leading to 100% insulin encapsulation and a high loading capability. The consecutive application of such coin-like MN patches successfully maintained plasma glucose level within the normal range for 48 h in both diabetic mice and minipigs [172]. Wang et al. further designed a dual-module MN patch to separately encapsulate insulin and glucagon, mimicking the counterregulatory effects of β and α cells in the pancreas (Figure 4a) [174]. The two modules were featured by different ratios of key monomers, hence, allowing a synergistic response in both hyperglycemia and hypoglycemia conditions [174]. For the second strategy, glucose oxidase (GOx) is frequently incorporated into nanoparticles as glucose sensors to modulate insulin release after microneedle application. GOx is able to catalyze glucose into gluconic acid with H_2O_2 as byproduct. Hence, the glucose-induced acidic or hypoxic microenvironment [175,176] and H_2O_2 [171,177,178] can be considered as stimuli to trigger insulin release. For example, hypoxia-sensitive hyaluronic acid vesicles containing insulin and GOx were incorporated into MN to achieve fast responsiveness to high glucose level (Figure 4b) [179]. Further research work suggested preloading Co^{2+} in MNs to catalyze the decomposition of the harmful byproduct H_2O_2 (Figure 4c) [175].
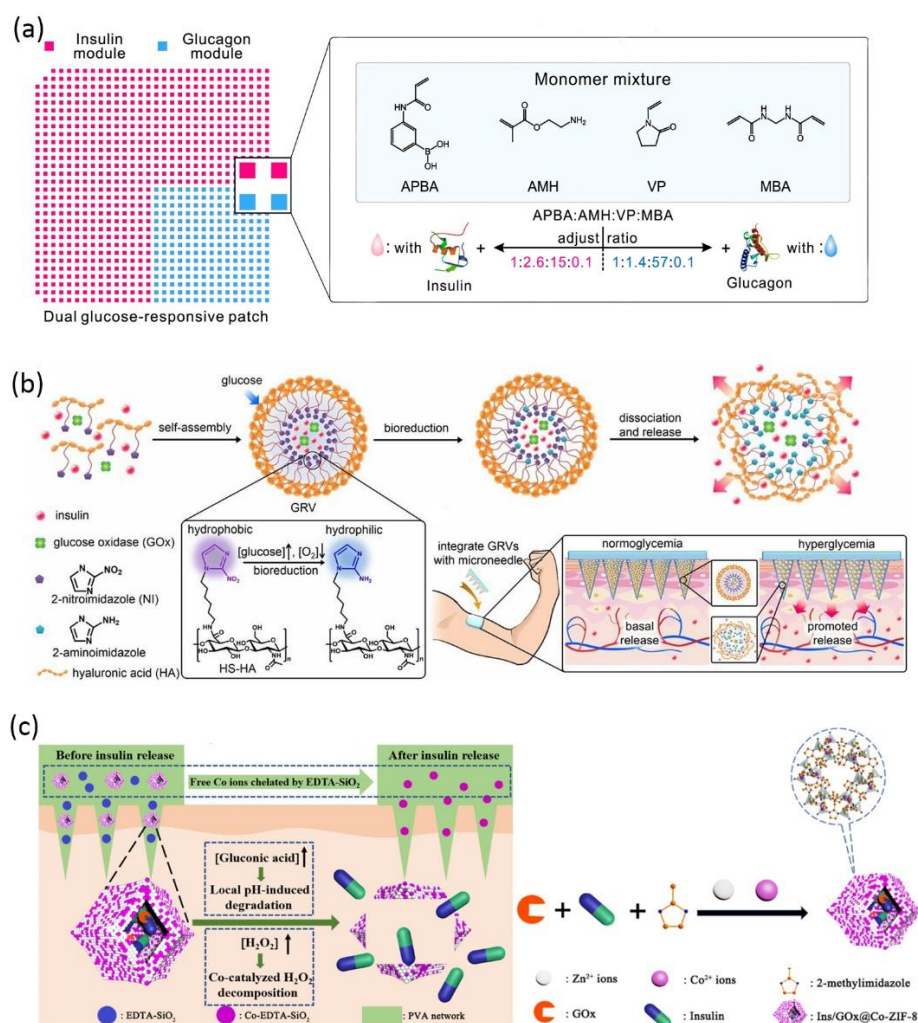
Figure 4. Schematic of glucose-responsive insulin delivery microneedles: (**a**) A dual-module microneedle patch to separately encapsulate insulin and glucagon. The two modules comprise different ratios of key monomers, synergistically responding to both hyperglycemic and hypoglycemic states (reproduced with permission from Wang et al., Proceedings of the National Academy of Sciences of the United States of America; published by National Academy of Sciences, 2020) [174]; (**b**) fast-responsive MN patch loaded with hypoxia-sensitive hyaluronic acid (HS-HA) vesicles containing insulin and GOx. In localized hypoxic environment, the hydrophobic 2-nitroimidazole groups of HS-HA are reduced to hydrophilic 2-aminoimdazole, leading to the dissociation of vesicles and subsequent release of insulin (reproduced with permission from Yu et al., Proceedings of the National Academy of Sciences of the United States of America; published by National Academy of Sciences, 2015) [179]; (**c**) the insulin and glucose oxidase are encapsulated in metal–organic framework and further loaded into the microneedle matrix. The low pH induced by glucose oxidation leads to framework degradation and insulin release. The preloaded Co^{2+} catalyzes the decomposition of the byproduct H_2O_2. The excessive Co^{2+} is chelated by EDTA-SiO_2 nanoparticles in the microneedle matrix (reproduced with permission from Yang et al., ACS Applied Materials & Interfaces; published by ACS, 2020) [176].

4. Outlook

The skin delivery of biomacromolecules has promising clinical relevance for both localized and systemic treatment. However, booming pre-clinical research contrasts with the sporadic clinical investigations. There stand a series of challenges to tackle for successful lab-to-market translation. Considering the labile nature of biological macromolecules, a detailed investigation regarding their stability during formulation preparation, as well as

different periods of storage, is necessary. Next, a dose regimen with high efficacy and low irritation should be screened. To this end, both drug-release behavior and pharmacokinetics should be systemically characterized. Unveiling the currently obscured mechanisms of different enhancers also contributes to more rational formulation design. In addition, extensive research should include the cumulative side effects associated with penetration enhancers and drug carrier materials. Eventually, scale-up production with low cost and prolonged shelf-life of biologics at room temperature are the key to gaining advantages in the pharmaceutical landscape.

Institutional Review Board Statement: Not applicable.

Informed Consent Statement: Not applicable.

Data Availability Statement: Data sharing not applicable.

Conflicts of Interest: The authors declare no conflict of interest.

References

1. Prausnitz, M.R.; Langer, R. Transdermal drug delivery. *Nat. Biotechnol.* **2008**, *26*, 1261–1268. [CrossRef]
2. Marwah, H.; Garg, T.; Goyal, A.K.; Rath, G. Permeation enhancer strategies in transdermal drug delivery. *Drug Deliv.* **2016**, *23*, 564–578. [CrossRef]
3. Borgheti-Cardoso, L.N.; Viegas, J.S.R.; Silvestrini, A.V.P.; Caron, A.L.; Praca, F.G.; Kravicz, M.; Bentley, M. Nanotechnology approaches in the current therapy of skin cancer. *Adv. Drug Deliv. Rev.* **2020**, *153*, 109–136. [CrossRef]
4. Willsmore, Z.N.; Coumbe, B.G.T.; Crescioli, S.; Reci, S.; Gupta, A.; Harris, R.J.; Chenoweth, A.; Chauhan, J.; Bax, H.J.; McCraw, A.; et al. Combined anti-PD-1 and anti-CTLA-4 checkpoint blockade: Treatment of melanoma and immune mechanisms of action. *Eur. J. Immunol.* **2021**, *51*, 544–556. [CrossRef]
5. Choi, J.U.; Lee, S.W.; Pangeni, R.; Byun, Y.; Yoon, I.S.; Park, J.W. Preparation and in vivo evaluation of cationic elastic liposomes comprising highly skin-permeable growth factors combined with hyaluronic acid for enhanced diabetic wound-healing therapy. *Acta Biomater.* **2017**, *57*, 197–215. [CrossRef]
6. Niu, Y.; Li, Q.; Ding, Y.; Dong, L.; Wang, C. Engineered delivery strategies for enhanced control of growth factor activities in wound healing. *Adv. Drug Deliv. Rev.* **2019**, *146*, 190–208. [CrossRef]
7. Laiva, A.L.; O'Brien, F.J.; Keogh, M.B. Innovations in gene and growth factor delivery systems for diabetic wound healing. *J. Tissue Eng. Regen. Med.* **2018**, *12*, e296–e312. [CrossRef]
8. Kanazawa, T.; Hamasaki, T.; Endo, T.; Tamano, K.; Sogabe, K.; Seta, Y.; Ohgi, T.; Okada, H. Functional peptide nanocarriers for delivery of novel anti-RelA RNA interference agents as a topical treatment of atopic dermatitis. *Int. J. Pharm.* **2015**, *489*, 261–267. [CrossRef]
9. Dharamdasani, V.; Mandal, A.; Qi, Q.M.; Suzuki, I.; Bentley, M.; Mitragotri, S. Topical delivery of siRNA into skin using ionic liquids. *J. Control. Release* **2020**, *323*, 475–482. [CrossRef]
10. Mandal, A.; Kumbhojkar, N.; Reilly, C.; Dharamdasani, V.; Ukidve, A.; Ingber, D.E.; Mitragotri, S. Treatment of psoriasis with NFKBIZ siRNA using topical ionic liquid formulations. *Sci. Adv.* **2020**, *6*, eabb6049. [CrossRef]
11. Liu, H.; Kang, R.S.; Bagnowski, K.; Yu, J.M.; Radecki, S.; Daniel, W.L.; Anderson, B.R.; Nallagatla, S.; Schook, A.; Agarwal, R.; et al. Targeting the IL-17 Receptor Using Liposomal Spherical Nucleic Acids as Topical Therapy for Psoriasis. *J. Investig. Dermatol.* **2020**, *140*, 435–444.e4. [CrossRef]
12. Li, J.; Li, X.; Zhang, Y.; Zhou, X.K.; Yang, H.S.; Chen, X.C.; Wang, Y.S.; Wei, Y.Q.; Chen, L.J.; Hu, H.Z.; et al. Gene therapy for psoriasis in the K14-VEGF transgenic mouse model by topical transdermal delivery of interleukin-4 using ultradeformable cationic liposome. *J. Gene Med.* **2010**, *12*, 481–490. [CrossRef]
13. Ita, K. Transdermal delivery of vaccines-Recent progress and critical issues. *Biomed. Pharmacother.* **2016**, *83*, 1080–1088. [CrossRef]
14. Maheshwari, C.; Pandey, R.S.; Chaurasiya, A.; Kumar, A.; Selvam, D.T.; Prasad, G.B.; Dixit, V.K. Non-ionic surfactant vesicles mediated transcutaneous immunization against hepatitis B. *Int. Immunopharmacol.* **2011**, *11*, 1516–1522. [CrossRef]
15. Nagano, H.; Kawabata, M.; Sugita, G.; Tsuruhara, A.; Ohori, J.; Jimura, T.; Miyashita, K.; Kurono, Y.; Tomonaga, K.; Briles, D.E.; et al. Transcutaneous immunization with pneumococcal surface protein A in mice. *Laryngoscope* **2018**, *128*, E91–E96. [CrossRef]

16. Novotny, L.A.; Bakaletz, L.O. Transcutaneous immunization with a nontypeable Haemophilus influenzae dual adhesin-directed immunogen induces durable and boostable immunity. *Vaccine* **2020**, *38*, 2378–2386. [CrossRef]

17. Tyagi, R.K.; Garg, N.K.; Jadon, R.; Sahu, T.; Katare, O.P.; Dalai, S.K.; Awasthi, A.; Marepally, S.K. Elastic liposome-mediated transdermal immunization enhanced the immunogenicity of P. falciparum surface antigen, MSP-119. *Vaccine* **2015**, *33*, 4630–4638. [CrossRef]

18. Duong, H.T.T.; Yin, Y.; Thambi, T.; Kim, B.S.; Jeong, J.H.; Lee, D.S. Highly potent intradermal vaccination by an array of dissolving microneedle polypeptide cocktails for cancer immunotherapy. *J. Mater. Chem. B* **2020**, *8*, 1171–1181. [CrossRef]

19. Zeng, Q.; Gammon, J.M.; Tostanoski, L.H.; Chiu, Y.C.; Jewell, C.M. In Vivo Expansion of Melanoma-Specific T Cells Using Microneedle Arrays Coated with Immune-Polyelectrolyte Multilayers. *ACS Biomater. Sci. Eng.* **2017**, *3*, 195–205. [CrossRef]

20. Kim, H.; Seong, K.Y.; Lee, J.H.; Park, W.; Yang, S.Y.; Hahn, S.K. Biodegradable Microneedle Patch Delivering Antigenic Peptide-Hyaluronate Conjugate for Cancer Immunotherapy. *ACS Biomater. Sci. Eng.* **2019**, *5*, 5150–5158. [CrossRef]

21. van der Maaden, K.; Varypataki, E.M.; Romeijn, S.; Ossendorp, F.; Jiskoot, W.; Bouwstra, J. Ovalbumin-coated pH-sensitive microneedle arrays effectively induce ovalbumin-specific antibody and T-cell responses in mice. *Eur. J. Pharm. Biopharm.* **2014**, *88*, 310–315. [CrossRef]

22. Tawde, S.A.; Chablani, L.; Akalkotkar, A.; D'Souza, M.J. Evaluation of microparticulate ovarian cancer vaccine via transdermal route of delivery. *J. Control. Release* **2016**, *235*, 147–154. [CrossRef]

23. Ye, Y.; Wang, C.; Zhang, X.; Hu, Q.; Zhang, Y.; Liu, Q.; Wen, D.; Milligan, J.; Bellotti, A.; Huang, L.; et al. A melanin-mediated cancer immunotherapy patch. *Sci. Immunol.* **2017**, *2*, eaan5692. [CrossRef]

24. Meneveau, M.O.; Petroni, G.R.; Salerno, E.P.; Lynch, K.T.; Smolkin, M.; Woodson, E.; Chianese-Bullock, K.A.; Olson, W.C.; Deacon, D.; Patterson, J.W.; et al. Immunogenicity in humans of a transdermal multipeptide melanoma vaccine administered with or without a TLR7 agonist. *J. Immunother. Cancer* **2021**, *9*, e002214. [CrossRef]

25. Lipinski, C.A. Lead- and drug-like compounds: The rule-of-five revolution. *Drug Discov. Today Technol.* **2004**, *1*, 337–341. [CrossRef]

26. Choy, Y.B.; Prausnitz, M.R. The rule of five for non-oral routes of drug delivery: Ophthalmic, inhalation and transdermal. *Pharm. Res.* **2011**, *28*, 943–948. [CrossRef]

27. Bolzinger, M.-A.; Briançon, S.; Pelletier, J.; Chevalier, Y. Penetration of drugs through skin, a complex rate-controlling membrane. *Curr. Opin. Colloid Interface Sci.* **2012**, *17*, 156–165. [CrossRef]

28. Anselmo, A.C.; Gokarn, Y.; Mitragotri, S. Non-invasive delivery strategies for biologics. *Nat. Rev. Drug Discov.* **2019**, *18*, 19–40. [CrossRef]

29. Zhu, Q.; Chen, Z.; Paul, P.K.; Lu, Y.; Wu, W.; Qi, J. Oral delivery of proteins and peptides: Challenges, status quo and future perspectives. *Acta Pharm. Sin. B* **2021**, *11*, 2416–2448. [CrossRef]

30. Gupta, R.; Dwadasi, B.S.; Rai, B.; Mitragotri, S. Effect of Chemical Permeation Enhancers on Skin Permeability: In silico screening using Molecular Dynamics simulations. *Sci. Rep.* **2019**, *9*, 1456. [CrossRef]

31. Kováčik, A.; Kopečná, M.; Vávrová, K. Permeation enhancers in transdermal drug delivery: Benefits and limitations. *Expert Opin. Drug Deliv.* **2020**, *17*, 145–155. [CrossRef] [PubMed]

32. Wong, T.W. Electrical, magnetic, photomechanical and cavitational waves to overcome skin barrier for transdermal drug delivery. *J. Control. Release* **2014**, *193*, 257–269. [CrossRef] [PubMed]

33. Munch, S.; Wohlrab, J.; Neubert, R.H.H. Dermal and transdermal delivery of pharmaceutically relevant macromolecules. *Eur. J. Pharm. Biopharm.* **2017**, *119*, 235–242. [CrossRef] [PubMed]

34. Baroni, A.; Buommino, E.; De Gregorio, V.; Ruocco, E.; Ruocco, V.; Wolf, R. Structure and function of the epidermis related to barrier properties. *Clin. Dermatol.* **2012**, *30*, 257–262. [CrossRef]

35. Crawford, M.; Dagnino, L. Scaffolding proteins in the development and maintenance of the epidermal permeability barrier. *Tissue Barriers* **2017**, *5*, e1341969. [CrossRef]

36. Gorzelanny, C.; Mess, C.; Schneider, S.W.; Huck, V.; Brandner, J.M. Skin Barriers in Dermal Drug Delivery: Which Barriers Have to Be Overcome and How Can We Measure Them? *Pharmaceutics* **2020**, *12*, 684. [CrossRef]

37. Notman, R.; Anwar, J. Breaching the skin barrier—Insights from molecular simulation of model membranes. *Adv. Drug Deliv. Rev.* **2013**, *65*, 237–250. [CrossRef]

38. Tsakovska, I.; Pajeva, I.; Al Sharif, M.; Alov, P.; Fioravanzo, E.; Kovarich, S.; Worth, A.P.; Richarz, A.N.; Yang, C.; Mostrag-Szlichtyng, A.; et al. Quantitative structure-skin permeability relationships. *Toxicology* **2017**, *387*, 27–42. [CrossRef]

39. Osseiran, S.; Cruz, J.D.; Jeong, S.; Wang, H.; Fthenakis, C.; Evans, C.L. Characterizing stratum corneum structure, barrier function, and chemical content of human skin with coherent Raman scattering imaging. *Biomed. Opt. Express* **2018**, *9*, 6425–6443. [CrossRef]

40. Kubo, A.; Ishizaki, I.; Kubo, A.; Kawasaki, H.; Nagao, K.; Ohashi, Y.; Amagai, M. The stratum corneum comprises three layers with distinct metal-ion barrier properties. *Sci. Rep.* **2013**, *3*, 1–11. [CrossRef]

41. Elias, P.M. Structure and function of the stratum corneum extracellular matrix. *J. Investig. Dermatol.* **2012**, *132*, 2131–2133. [CrossRef] [PubMed]

42. van Smeden, J.; Hoppel, L.; van der Heijden, R.; Hankemeier, T.; Vreeken, R.J.; Bouwstra, J.A. LC/MS analysis of stratum corneum lipids: Ceramide profiling and discovery. *J. Lipid Res.* **2011**, *52*, 1211–1221. [CrossRef]

43. Yarovoy, Y.; Drutis, D.M.; Hancewicz, T.M.; Garczarek, U.; Ananthapadmanabhan, K.P.; Misra, M. Quantification of Lipid Phase Order of In Vivo Human Skin Using Attenuated Total Reflection Fourier Transform Infrared (ATR FT-IR) Spectroscopy and Multivariate Curve Resolution Analysis. *Appl. Spectrosc.* **2019**, *73*, 182–194. [CrossRef] [PubMed]

44. Haftek, M. Epidermal barrier disorders and corneodesmosome defects. *Cell Tissue Res.* **2014**, *360*, 483–490. [CrossRef] [PubMed]

45. Kirschner, N.; Rosenthal, R.; Furuse, M.; Moll, I.; Fromm, M.; Brandner, J.M. Contribution of tight junction proteins to ion, macromolecule, and water barrier in keratinocytes. *J. Investig. Dermatol.* **2013**, *133*, 1161–1169. [CrossRef]

46. Basler, K.; Bergmann, S.; Heisig, M.; Naegel, A.; Zorn-Kruppa, M.; Brandner, J.M. The role of tight junctions in skin barrier function and dermal absorption. *J. Control. Release* **2016**, *242*, 105–118. [CrossRef]

47. Umeda, K.; Ikenouchi, J.; Katahira-Tayama, S.; Furuse, K.; Sasaki, H.; Nakayama, M.; Matsui, T.; Tsukita, S.; Furuse, M.; Tsukita, S. ZO-1 and ZO-2 independently determine where claudins are polymerized in tight-junction strand formation. *Cell* **2006**, *126*, 741–754. [CrossRef]

48. Sugawara, T.; Iwamoto, N.; Akashi, M.; Kojima, T.; Hisatsune, J.; Sugai, M.; Furuse, M. Tight junction dysfunction in the stratum granulosum leads to aberrant stratum corneum barrier function in claudin-1-deficient mice. *J. Dermatol. Sci.* **2013**, *70*, 12–18. [CrossRef]

49. Arda, O.; Göksügür, N.; Tüzün, Y. Basic histological structure and functions of facial skin. *Clin. Dermatol.* **2014**, *32*, 3–13. [CrossRef]

50. Jacobi, U.; Engel, K.; Patzelt, A.; Worm, M.; Sterry, W.; Lademann, J. Penetration of pollen proteins into the skin. *Skin Pharmacol. Physiol.* **2007**, *20*, 297–304. [CrossRef]

51. Meinke, M.C.; Patzelt, A.; Richter, H.; Schanzer, S.; Sterry, W.; Filbry, A.; Bohnsack, K.; Rippke, F.; Galecka, J.; Fölster-Holst, R.; et al. Prevention of follicular penetration: Barrier-enhancing formulations against the penetration of pollen allergens into hair follicles. *Skin Pharmacol. Physiol.* **2011**, *24*, 144–150. [CrossRef] [PubMed]

52. Lademann, J.; Richter, H.; Meinke, M.; Sterry, W.; Patzelt, A. Which skin model is the most appropriate for the investigation of topically applied substances into the hair follicles? *Skin Pharmacol. Physiol.* **2010**, *23*, 47–52. [CrossRef] [PubMed]

53. Zorn-Kruppa, M.; Vidal, Y.S.S.; Houdek, P.; Wladykowski, E.; Grzybowski, S.; Gruber, R.; Gorzelanny, C.; Harcup, J.; Schneider, S.W.; Majumdar, A.; et al. Tight Junction barriers in human hair follicles-role of claudin-1. *Sci. Rep.* **2018**, *8*, 12800. [CrossRef] [PubMed]

54. Beier, L.S.; Rossa, J.; Woodhouse, S.; Bergmann, S.; Kramer, H.B.; Protze, J.; Eichner, M.; Piontek, A.; Vidal, Y.S.S.; Brandner, J.M.; et al. Use of Modified Clostridium perfringens Enterotoxin Fragments for Claudin Targeting in Liver and Skin Cells. *Int. J. Mol. Sci.* **2019**, *20*, 4774. [CrossRef] [PubMed]

55. Banerjee, A.; Ibsen, K.; Iwao, Y.; Zakrewsky, M.; Mitragotri, S. Transdermal Protein Delivery Using Choline and Geranate (CAGE) Deep Eutectic Solvent. *Adv. Healthc. Mater.* **2017**, *6*, 1601411. [CrossRef]

56. Madani, F.; Gräslund, A. Membrane Molecular Interactions and Induced Structures of CPPs. *Methods Mol. Biol.* **2022**, *2383*, 153–165. [CrossRef]

57. Roberts, M.S.; Mohammed, Y.; Pastore, M.N.; Namjoshi, S.; Yousef, S.; Alinaghi, A.; Haridass, I.N.; Abd, E.; Leite-Silva, V.R.; Benson, H.; et al. Topical and cutaneous delivery using nanosystems. *J. Control. Release.* **2017**, *247*, 86–105. [CrossRef]

58. Yang, J.; Liu, X.; Fu, Y.; Song, Y. Recent advances of microneedles for biomedical applications: Drug delivery and beyond. *Acta Pharm. Sin. B* **2019**, *9*, 469–483. [CrossRef]

59. Egorova, K.S.; Gordeev, E.G.; Ananikov, V.P. Biological Activity of Ionic Liquids and Their Application in Pharmaceutics and Medicine. *Chem. Rev.* **2017**, *117*, 7132–7189. [CrossRef]

60. Huang, W.; Wu, X.; Qi, J.; Zhu, Q.; Wu, W.; Lu, Y.; Chen, Z. Ionic liquids: Green and tailor-made solvents in drug delivery. *Drug Discov. Today* **2019**, *25*, 901–908. [CrossRef]

61. Banerjee, A.; Ibsen, K.; Brown, T.; Chen, R.; Agatemor, C.; Mitragotri, S. Reply to Rogers and Gurau: Definitions of ionic liquids and deep eutectic solvents. *Proc. Natl. Acad. Sci. USA* **2018**, *115*, E11000–E11001. [CrossRef] [PubMed]

62. Jesus, A.R.; Soromenho, M.R.C.; Raposo, L.R.; Esperanca, J.; Baptista, P.V.; Fernandes, A.R.; Reis, P.M. Enhancement of water solubility of poorly water-soluble drugs by new biocompatible N-acetyl amino acid N-alkyl cholinium-based ionic liquids. *Eur. J. Pharm. Biopharm.* **2019**, *137*, 227–232. [CrossRef] [PubMed]

63. Zakrewsky, M.; Banerjee, A.; Apte, S.; Kern, T.L.; Jones, M.R.; Sesto, R.E.; Koppisch, A.T.; Fox, D.T.; Mitragotri, S. Choline and Geranate Deep Eutectic Solvent as a Broad-Spectrum Antiseptic Agent for Preventive and Therapeutic Applications. *Adv. Healthc. Mater.* **2016**, *5*, 1282–1289. [CrossRef] [PubMed]

64. Jorge, L.R.; Harada, L.K.; Silva, E.C.; Campos, W.F.; Moreli, F.C.; Shimamoto, G.; Pereira, J.F.B.; Oliveira, J.M., Jr.; Tubino, M.; Vila, M.; et al. Non-invasive Transdermal Delivery of Human Insulin Using Ionic Liquids: In vitro Studies. *Front. Pharmacol.* **2020**, *11*, 243. [CrossRef]

65. Qi, Q.M.; Mitragotri, S. Mechanistic study of transdermal delivery of macromolecules assisted by ionic liquids. *J. Control. Release* **2019**, *311*, 162–169. [CrossRef]

66. Wu, X.; Chen, Z.; Li, Y.; Yu, Q.; Lu, Y.; Zhu, Q.; Li, Y.; An, D.; Qi, J.; Wu, W. Improving dermal delivery of hydrophilic macromolecules by biocompatible ionic liquid based on choline and malic acid. *Int. J. Pharm.* **2019**, *558*, 380–387. [CrossRef]

67. Wu, X.; Zhang, H.; He, S.; Yu, Q.; Lu, Y.; Wu, W.; Ding, N.; Zhu, Q.; Chen, Z.; Ma, Y.; et al. Improving dermal delivery of hyaluronic acid by ionic liquids for attenuating skin dehydration. *Int. J. Biol. Macromol.* **2020**, *150*, 528–535. [CrossRef]

68. Zakrewsky, M.; Mitragotri, S. Therapeutic RNAi robed with ionic liquid moieties as a simple, scalable prodrug platform for treating skin disease. *J. Control. Release* **2016**, *242*, 80–88. [CrossRef]

69. Tahara, Y.; Morita, K.; Wakabayashi, R.; Kamiya, N.; Goto, M. Biocompatible Ionic Liquid Enhances Transdermal Antigen Peptide Delivery and Preventive Vaccination Effect. *Mol. Pharm.* **2020**, *17*, 3845–3856. [CrossRef]

70. Islam, M.R.; Uddin, S.; Chowdhury, M.R.; Wakabayashi, R.; Moniruzzaman, M.; Goto, M. Insulin Transdermal Delivery System for Diabetes Treatment Using a Biocompatible Ionic Liquid-Based Microemulsion. *ACS Appl. Mater. Interfaces* **2021**, *13*, 42461–42472. [CrossRef]

71. Chowdhury, M.R.; Moshikur, R.M.; Wakabayashi, R.; Moniruzzaman, M.; Goto, M. Biocompatible ionic liquids assisted transdermal co-delivery of antigenic protein and adjuvant for cancer immunotherapy. *Int. J. Pharm.* **2021**, *601*, 120582. [CrossRef] [PubMed]

72. Kumar, A.; Venkatesu, P. Innovative aspects of protein stability in ionic liquid mixtures. *Biophys. Rev.* **2018**, *10*, 841–846. [CrossRef] [PubMed]

73. Mazid, R.R.; Divisekera, U.; Yang, W.; Ranganathan, V.; MacFarlane, D.R.; Cortez-Jugo, C.; Cheng, W. Biological stability and activity of siRNA in ionic liquids. *Chem. Commun.* **2014**, *50*, 13457–13460. [CrossRef] [PubMed]

74. Palanisamy, K.; Prakash, M. The molecular mechanism behind the stabilization of insulin by choline and geranate (CAGE) ionic liquids-computational insights into oral insulin drug formulation. *Phys. Chem. Chem. Phys.* **2021**, *23*, 25298–25307. [CrossRef]

75. Tanner, E.E.L.; Ibsen, K.N.; Mitragotri, S. Transdermal insulin delivery using choline-based ionic liquids (CAGE). *J. Control. Release* **2018**, *286*, 137–144. [CrossRef]

76. Wang, C.; Zhu, J.; Zhang, D.; Yang, Y.; Zheng, L.; Qu, Y.; Yang, X.; Cui, X. Ionic liquid-microemulsions assisting in the transdermal delivery of Dencichine: Preparation, in-vitro and in-vivo evaluations, and investigation of the permeation mechanism. *Int. J. Pharm.* **2018**, *535*, 120–131. [CrossRef]

77. Zheng, L.; Zhao, Z.; Yang, Y.; Li, Y.; Wang, C. Novel skin permeation enhancers based on amino acid ester ionic liquid: Design and permeation mechanism. *Int. J. Pharm.* **2020**, *576*, 119031. [CrossRef]

78. Takeda, J.; Iwao, Y.; Karashima, M.; Yamamoto, K.; Ikeda, Y. Structural Evaluation of the Choline and Geranic Acid/Water Complex by SAXS and NMR Analyses. *ACS Biomater. Sci. Eng.* **2021**, *7*, 595–604. [CrossRef]

79. Ruan, R.-q.; Wang, S.-s.; Wang, C.-l.; Zhang, L.; Zhang, Y.-j.; Zhou, W.; Ding, W.-p.; Jin, P.-p.; Wei, P.-f.; Man, N.; et al. Transdermal delivery of human epidermal growth factor facilitated by a peptide chaperon. *Eur. J. Med. Chem.* **2013**, *62*, 405–409. [CrossRef]

80. Xu, J.; Khan, A.R.; Fu, M.; Wang, R.; Ji, J.; Zhai, G. Cell-penetrating peptide: A means of breaking through the physiological barriers of different tissues and organs. *J. Control. Release* **2019**, *309*, 106–124. [CrossRef]

81. Copolovici, D.M.; Langel, K.; Eriste, E.; Langel, Ü. Cell-Penetrating Peptides: Design, Synthesis, and Applications. *ACS Nano* **2014**, *8*, 1972–1994. [CrossRef] [PubMed]

82. Gan, B.K.; Yong, C.Y.; Ho, K.L.; Omar, A.R.; Alitheen, N.B.; Tan, W.S. Targeted Delivery of Cell Penetrating Peptide Virus-like Nanoparticles to Skin Cancer Cells. *Sci. Rep.* **2018**, *8*, 8499. [CrossRef] [PubMed]

83. Ezzat, K.; Andaloussi, S.E.; Zaghloul, E.M.; Lehto, T.; Lindberg, S.; Moreno, P.M.; Viola, J.R.; Magdy, T.; Abdo, R.; Guterstam, P.; et al. PepFect 14, a novel cell-penetrating peptide for oligonucleotide delivery in solution and as solid formulation. *Nucleic Acids Res.* **2011**, *39*, 5284–5298. [CrossRef] [PubMed]

84. Bode, S.A.; Wallbrecher, R.; Brock, R.; van Hest, J.C.; Löwik, D.W. Activation of cell-penetrating peptides by disulfide bridge formation of truncated precursors. *Chem. Commun.* **2014**, *50*, 415–417. [CrossRef] [PubMed]

85. Mandal, D.; Nasrolahi Shirazi, A.; Parang, K. Cell-penetrating homochiral cyclic peptides as nuclear-targeting molecular transporters. *Angew. Chem. Int. Ed.* **2011**, *50*, 9633–9637. [CrossRef] [PubMed]

86. Im, J.; Das, S.; Jeong, D.; Kim, C.J.; Lim, H.S.; Kim, K.H.; Chung, S.K. Intracellular and transdermal protein delivery mediated by non-covalent interactions with a synthetic guanidine-rich molecular carrier. *Int. J. Pharm.* **2017**, *528*, 646–654. [CrossRef]

87. Chen, Y.; Shen, Y.; Guo, X.; Zhang, C.; Yang, W.; Ma, M.; Liu, S.; Zhang, M.; Wen, L.-P. Transdermal protein delivery by a coadministered peptide identified via phage display. *Nat. Biotechnol.* **2006**, *24*, 455–460. [CrossRef]

88. Kristensen, M.; Birch, D.; Morck Nielsen, H. Applications and Challenges for Use of Cell-Penetrating Peptides as Delivery Vectors for Peptide and Protein Cargos. *Int. J. Mol. Sci.* **2016**, *17*, 185. [CrossRef]

89. Gautam, A.; Nanda, J.S.; Samuel, J.S.; Kumari, M.; Priyanka, P.; Bedi, G.; Nath, S.K.; Mittal, G.; Khatri, N.; Raghava, G.P.S. Topical Delivery of Protein and Peptide Using Novel Cell Penetrating Peptide IMT-P8. *Sci. Rep.* **2016**, *6*, 1–13. [CrossRef]

90. Ruan, R.; Chen, M.; Sun, S.; Wei, P.; Zou, L.; Liu, J.; Gao, D.; Wen, L.; Ding, W. Topical and Targeted Delivery of siRNAs to Melanoma Cells Using a Fusion Peptide Carrier. *Sci. Rep.* **2016**, *6*, 29159. [CrossRef]

91. Derossi, D.; Chassaing, G.; Prochiantz, A. Trojan peptides: The penetratin system for intracellular delivery. *Trends Cell Biol.* **1998**, *8*, 84–87. [CrossRef]

92. Pouny, Y.; Rapaport, D.; Mor, A.; Nicolas, P.; Shai, Y. Interaction of antimicrobial dermaseptin and its fluorescently labeled analogues with phospholipid membranes. *Biochemistry* **1992**, *31*, 12416–12423. [CrossRef] [PubMed]

93. Moghal, M.M.R.; Shuma, M.L.; Islam, M.Z.; Yamazaki, M. A Single GUV Method for Revealing the Action of Cell-Penetrating Peptides in Biomembranes. *Methods Mol. Biol.* **2022**, *2383*, 167–179. [CrossRef]

94. Ruseska, I.; Zimmer, A. Internalization mechanisms of cell-penetrating peptides. *Beilstein J. Nanotechnol.* **2020**, *11*, 101–123. [CrossRef]

95. Zorko, M.; Langel, Ü. Cell-Penetrating Peptides. *Methods Mol. Biol.* **2022**, *2383*, 3–32. [CrossRef] [PubMed]

96. de Jong, H.; Bonger, K.M.; Löwik, D. Activatable cell-penetrating peptides: 15 years of research. *RSC Chem. Biol* **2020**, *1*, 192–203. [CrossRef] [PubMed]

97. Nor Azlan, A.Y.H.; Katas, H.; Mohamad Zin, N.; Fauzi, M.B. Dual action gels containing DsiRNA loaded gold nanoparticles: Augmenting diabetic wound healing by promoting angiogenesis and inhibiting infection. *Eur. J. Pharm. Biopharm* **2021**, *169*, 78–90. [CrossRef]

98. Niu, J.; Chu, Y.; Huang, Y.F.; Chong, Y.S.; Jiang, Z.H.; Mao, Z.W.; Peng, L.H.; Gao, J.Q. Transdermal Gene Delivery by Functional Peptide-Conjugated Cationic Gold Nanoparticle Reverses the Progression and Metastasis of Cutaneous Melanoma. *ACS Appl. Mater. Interfaces* **2017**, *9*, 9388–9401. [CrossRef]

99. Nemati, H.; Ghahramani, M.H.; Faridi-Majidi, R.; Izadi, B.; Bahrami, G.; Madani, S.H.; Tavoosidana, G. Using siRNA-based spherical nucleic acid nanoparticle conjugates for gene regulation in psoriasis. *J. Control. Release* **2017**, *268*, 259–268. [CrossRef]

100. Randeria, P.S.; Seeger, M.A.; Wang, X.Q.; Wilson, H.; Shipp, D.; Mirkin, C.A.; Paller, A.S. siRNA-based spherical nucleic acids reverse impaired wound healing in diabetic mice by ganglioside GM_3 synthase knockdown. *Proc. Natl. Acad. Sci. USA* **2015**, *112*, 5573–5578. [CrossRef]

101. Wang, S.; Yan, C.; Zhang, X.; Shi, D.; Chi, L.; Luo, G.; Deng, J. Antimicrobial peptide modification enhances the gene delivery and bactericidal efficiency of gold nanoparticles for accelerating diabetic wound healing. *Biomater. Sci.* **2018**, *6*, 2757–2772. [CrossRef] [PubMed]

102. Chen, Y.; Wu, Y.; Gao, J.; Zhang, Z.; Wang, L.; Chen, X.; Mi, J.; Yao, Y.; Guan, D.; Chen, B.; et al. Transdermal Vascular Endothelial Growth Factor Delivery with Surface Engineered Gold Nanoparticles. *ACS Appl. Mater. Interfaces* **2017**, *9*, 5173–5180. [CrossRef] [PubMed]

103. Pan, A.; Zhong, M.; Wu, H.; Peng, Y.; Xia, H.; Tang, Q.; Huang, Q.; Wei, L.; Xiao, L.; Peng, C. Topical Application of Keratinocyte Growth Factor Conjugated Gold Nanoparticles Accelerate Wound Healing. *Nanomedicine* **2018**, *14*, 1619–1628. [CrossRef]

104. Huang, Y.; Yu, F.; Park, Y.S.; Wang, J.; Shin, M.C.; Chung, H.S.; Yang, V.C. Co-administration of protein drugs with gold nanoparticles to enable percutaneous delivery. *Biomaterials* **2010**, *31*, 9086–9091. [CrossRef] [PubMed]

105. Casciaro, B.; Moros, M.; Rivera-Fernández, S.; Bellelli, A.; de la Fuente, J.M.; Mangoni, M.L. Gold-nanoparticles coated with the antimicrobial peptide esculentin-1a(1-21)NH_2 as a reliable strategy for antipseudomonal drugs. *Acta Biomater.* **2017**, *47*, 170–181. [CrossRef] [PubMed]

106. Siu, K.S.; Chen, D.; Zheng, X.; Zhang, X.; Johnston, N.; Liu, Y.; Yuan, K.; Koropatnick, J.; Gillies, E.R.; Min, W.P. Non-covalently functionalized single-walled carbon nanotube for topical siRNA delivery into melanoma. *Biomaterials* **2014**, *35*, 3435–3442. [CrossRef] [PubMed]

107. Lio, D.C.S.; Liu, C.; Oo, M.M.S.; Wiraja, C.; Teo, M.H.Y.; Zheng, M.; Chew, S.W.T.; Wang, X.; Xu, C. Transdermal delivery of small interfering RNAs with topically applied mesoporous silica nanoparticles for facile skin cancer treatment. *Nanoscale* **2019**, *11*, 17041–17051. [CrossRef]

108. Viegas, J.S.R.; Praca, F.G.; Caron, A.L.; Suzuki, I.; Silvestrini, A.V.P.; Medina, W.S.G.; Del Ciampo, J.O.; Kravicz, M.; Bentley, M. Nanostructured lipid carrier co-delivering tacrolimus and TNF-alpha siRNA as an innovate approach to psoriasis. *Drug Deliv. Transl. Res.* **2020**, *10*, 646–660. [CrossRef]

109. Rabbani, P.S.; Zhou, A.; Borab, Z.M.; Frezzo, J.A.; Srivastava, N.; More, H.T.; Rifkin, W.J.; David, J.A.; Berens, S.J.; Chen, R.; et al. Novel lipoproteoplex delivers Keap1 siRNA based gene therapy to accelerate diabetic wound healing. *Biomaterials* **2017**, *132*, 1–15. [CrossRef]

110. Desmet, E.; Bracke, S.; Forier, K.; Taevernier, L.; Stuart, M.C.; De Spiegeleer, B.; Raemdonck, K.; Van Gele, M.; Lambert, J. An elastic liposomal formulation for RNAi-based topical treatment of skin disorders: Proof-of-concept in the treatment of psoriasis. *Int. J. Pharm.* **2016**, *500*, 268–274. [CrossRef]

111. Chaudhari, R.; Tandel, N.; Sahu, K.; Negi, S.; Bashir, H.; Rupareliya, A.; Mishra, R.P.; Dalai, S.K.; Tyagi, R.K. Transdermal Immunization of Elastic Liposome-Laden Recombinant Chimeric Fusion Protein of P. falciparum (PfMSP-Fu$_{24}$) Mounts Protective Immune Response. *Nanomaterials* **2021**, *11*, 406. [CrossRef] [PubMed]

112. Bracke, S.; Carretero, M.; Guerrero-Aspizua, S.; Desmet, E.; Illera, N.; Navarro, M.; Lambert, J.; Del Rio, M. Targeted silencing of DEFB$_4$ in a bioengineered skin-humanized mouse model for psoriasis: Development of siRNA SECosome-based novel therapies. *Exp. Dermatol.* **2014**, *23*, 199–201. [CrossRef] [PubMed]

113. Wang, J.; Hu, J.H.; Li, F.Q.; Liu, G.Z.; Zhu, Q.G.; Liu, J.Y.; Ma, H.J.; Peng, C.; Si, F.G. Strong cellular and humoral immune responses induced by transcutaneous immunization with HBsAg DNA-cationic deformable liposome complex. *Exp. Dermatol.* **2007**, *16*, 724–729. [CrossRef] [PubMed]

114. Vyas, S.P.; Singh, R.P.; Jain, S.; Mishra, V.; Mahor, S.; Singh, P.; Gupta, P.N.; Rawat, A.; Dubey, P. Non-ionic surfactant based vesicles (niosomes) for non-invasive topical genetic immunization against hepatitis B. *Int. J. Pharm.* **2005**, *296*, 80–86. [CrossRef]

115. Chen, M.; Zakrewsky, M.; Gupta, V.; Anselmo, A.C.; Slee, D.H.; Muraski, J.A.; Mitragotri, S. Topical delivery of siRNA into skin using SPACE-peptide carriers. *J. Control. Release* **2014**, *179*, 33–41. [CrossRef]

116. Marepally, S.; Boakye, C.H.; Patel, A.R.; Godugu, C.; Doddapaneni, R.; Desai, P.R.; Singh, M. Topical administration of dual siRNAs using fusogenic lipid nanoparticles for treating psoriatic-like plaques. *Nanomedicine* **2014**, *9*, 2157–2174. [CrossRef]

117. Kasiewicz, L.N.; Whitehead, K.A. Lipid nanoparticles silence tumor necrosis factor α to improve wound healing in diabetic mice. *Bioeng. Transl. Med.* **2019**, *4*, 75–82. [CrossRef]

118. Garcia-Orue, I.; Gainza, G.; Girbau, C.; Alonso, R.; Aguirre, J.J.; Pedraz, J.L.; Igartua, M.; Hernandez, R.M. LL$_{37}$ loaded nanostructured lipid carriers (NLC): A new strategy for the topical treatment of chronic wounds. *Eur. J. Pharm. Biopharm.* **2016**, *108*, 310–316. [CrossRef]

119. Gainza, G.; Bonafonte, D.C.; Moreno, B.; Aguirre, J.J.; Gutierrez, F.B.; Villullas, S.; Pedraz, J.L.; Igartua, M.; Hernandez, R.M. The topical administration of rhEGF-loaded nanostructured lipid carriers (rhEGF-NLC) improves healing in a porcine full-thickness excisional wound model. *J. Control. Release* **2015**, *197*, 41–47. [CrossRef]

120. Desai, P.R.; Marepally, S.; Patel, A.R.; Voshavar, C.; Chaudhuri, A.; Singh, M. Topical delivery of anti-TNFalpha siRNA and capsaicin via novel lipid-polymer hybrid nanoparticles efficiently inhibits skin inflammation in vivo. *J. Control. Release* **2013**, *170*, 51–63. [CrossRef]

121. Suzuki, I.L.; de Araujo, M.M.; Bagnato, V.S.; Bentley, M. TNFalpha siRNA delivery by nanoparticles and photochemical internalization for psoriasis topical therapy. *J. Control. Release* **2021**, *338*, 316–329. [CrossRef] [PubMed]

122. Tofani, L.B.; Depieri, L.V.; Campos, P.M.; Riul, T.B.; Antonietto, K.S.; de Abreu Fantini, M.C.; Bentley, M. In Vitro TyRP-1 Knockdown Based on siRNA Carried by Liquid Crystalline Nanodispersions: An Alternative Approach for Topical Treatment of Vitiligo. *Pharm. Res.* **2018**, *35*, 104. [CrossRef] [PubMed]

123. Petrilli, R.; Eloy, J.O.; Praca, F.S.; Del Ciampo, J.O.; Fantini, M.A.; Fonseca, M.J.; Bentley, M.V. Liquid Crystalline Nanodispersions Functionalized with Cell-Penetrating Peptides for Topical Delivery of Short-Interfering RNAs: A Proposal for Silencing a Pro-Inflammatory Cytokine in Cutaneous Diseases. *J. Biomed. Nanotechnol.* **2016**, *12*, 1063–1075. [CrossRef] [PubMed]

124. Lopes, L.B.; Ferreira, D.A.; de Paula, D.; Garcia, M.T.; Thomazini, J.A.; Fantini, M.C.; Bentley, M.V. Reverse hexagonal phase nanodispersion of monoolein and oleic acid for topical delivery of peptides: In vitro and in vivo skin penetration of cyclosporin A. *Pharm. Res.* **2006**, *23*, 1332–1342. [CrossRef] [PubMed]

125. Depieri, L.V.; Borgheti-Cardoso, L.N.; Campos, P.M.; Otaguiri, K.K.; Vicentini, F.T.; Lopes, L.B.; Fonseca, M.J.; Bentley, M.V. RNAi mediated IL-6 in vitro knockdown in psoriasis skin model with topical siRNA delivery system based on liquid crystalline phase. *Eur. J. Pharm. Biopharm.* **2016**, *105*, 50–58. [CrossRef]

126. Boge, L.; Hallstensson, K.; Ringstad, L.; Johansson, J.; Andersson, T.; Davoudi, M.; Larsson, P.T.; Mahlapuu, M.; Håkansson, J.; Andersson, M. Cubosomes for topical delivery of the antimicrobial peptide LL-$_{37}$. *Eur. J. Pharm. Biopharm.* **2019**, *134*, 60–67. [CrossRef]

127. Bahadoran, A.; Moeini, H.; Bejo, M.H.; Hussein, M.Z.; Omar, A.R. Development of Tat-Conjugated Dendrimer for Transdermal DNA Vaccine Delivery. *J. Pharm. Pharm. Sci.* **2016**, *19*, 325–338. [CrossRef]

128. Alyoussef Alkrad, J.; Neubert, R.H.H. Dermal and transdermal peptide delivery using enhancer molecules and colloidal carrier systems. Part V: Transdermal administration of insulin. *Int. J. Pharm.* **2022**, *616*, 121511. [CrossRef]

129. Yun, S.I.; Lee, S.K.; Goh, E.A.; Kwon, O.S.; Choi, W.; Kim, J.; Lee, M.S.; Choi, S.J.; Lim, S.S.; Moon, T.K.; et al. Weekly treatment with SAMiRNA targeting the androgen receptor ameliorates androgenetic alopecia. *Sci. Rep.* **2022**, *12*, 1607. [CrossRef]

130. Akhter, K.F.; Mumin, M.A.; Lui, E.M.K.; Charpentier, P.A. Transdermal nanotherapeutics: Panax quinquefolium polysaccharide nanoparticles attenuate UVB-induced skin cancer. *Int. J. Biol. Macromol.* **2021**, *181*, 221–231. [CrossRef]

131. Zou, J.J.; Le, J.Q.; Zhang, B.C.; Yang, M.Y.; Jiang, J.L.; Lin, J.F.; Wu, P.Y.; Li, C.; Chen, L.; Shao, J.W. Accelerating transdermal delivery of insulin by ginsenoside nanoparticles with unique permeability. *Int. J. Pharm.* **2021**, *605*, 120784. [CrossRef] [PubMed]

132. Hartono, D.; Qin, W.J.; Yang, K.-L.; Yung, L.-Y.L. Imaging the disruption of phospholipid monolayer by protein-coated nanoparticles using ordering transitions of liquid crystals. *Biomaterials* **2009**, *30*, 843–849. [CrossRef] [PubMed]

133. Siu, K.S.; Zhang, Y.; Zheng, X.; Koropatnick, J.; Min, W.P. Non-Covalently Functionalized of Single-Walled Carbon Nanotubes by DSPE-PEG-PEI for SiRNA Delivery. *Methods Mol. Biol.* **2016**, *1364*, 151–163. [CrossRef] [PubMed]

134. Schlich, M.; Musazzi, U.M.; Campani, V.; Biondi, M.; Franze, S.; Lai, F.; De Rosa, G.; Sinico, C.; Cilurzo, F. Design and development of topical liposomal formulations in a regulatory perspective. *Drug Deliv. Transl. Res.* **2022**, *12*, 1811–1828. [CrossRef]

135. Cevc, G.; Schätzlein, A.; Blume, G. Transdermal drug carriers: Basic properties, optimization and transfer efficiency in the case of epicutaneously applied peptides. *J. Control. Release* **1995**, *36*, 3–16. [CrossRef]

136. Dorrani, M.; Garbuzenko, O.B.; Minko, T.; Michniak-Kohn, B. Development of edge-activated liposomes for siRNA delivery to human basal epidermis for melanoma therapy. *J. Control. Release* **2016**, *228*, 150–158. [CrossRef]

137. Babaie, S.; Bakhshayesh, A.R.D.; Ha, J.W.; Hamishehkar, H.; Kim, K.H. Invasome: A Novel Nanocarrier for Transdermal Drug Delivery. *Nanomaterials* **2020**, *10*, 341. [CrossRef]

138. Touitou, E.; Dayan, N.; Bergelson, L.; Godin, B.; Eliaz, M. Ethosomes-novel vesicular carriers for enhanced delivery: Characterization and skin penetration properties. *J. Control. Release* **2000**, *65*, 403–418. [CrossRef]

139. Jijie, R.; Barras, A.; Boukherroub, R.; Szunerits, S. Nanomaterials for transdermal drug delivery: Beyond the state of the art of liposomal structures. *J. Mater. Chem. B* **2017**, *5*, 8653–8675. [CrossRef]

140. Vicentini, F.T.; Depieri, L.V.; Polizello, A.C.; Del Ciampo, J.O.; Spadaro, A.C.; Fantini, M.C.; Vitoria Lopes Badra Bentley, M. Liquid crystalline phase nanodispersions enable skin delivery of siRNA. *Eur. J. Pharm. Biopharm.* **2013**, *83*, 16–24. [CrossRef]

141. Chen, Y.; Wang, M.; Fang, L. Biomaterials as novel penetration enhancers for transdermal and dermal drug delivery systems. *Drug Deliv.* **2013**, *20*, 199–209. [CrossRef] [PubMed]

142. Bahadoran, A.; Ebrahimi, M.; Yeap, S.K.; Safi, N.; Moeini, H.; Hair-Bejo, M.; Hussein, M.Z.; Omar, A.R. Induction of a robust immune response against avian influenza virus following transdermal inoculation with H5-DNA vaccine formulated in modified dendrimer-based delivery system in mouse model. *Int. J. Nanomed.* **2017**, *12*, 8573–8585. [CrossRef] [PubMed]

143. Sun, M.; Fan, A.; Wang, Z.; Zhao, Y. Dendrimer-mediated drug delivery to the skin. *Soft Matter* **2012**, *8*, 4301–4305. [CrossRef]
144. Sharma, S.; Hatware, K.; Bhadane, P.; Sindhikar, S.; Mishra, D.K. Recent advances in microneedle composites for biomedical applications: Advanced drug delivery technologies. *Mater. Sci. Eng. C Mater. Biol. Appl.* **2019**, *103*, 109717. [CrossRef]
145. Wang, M.; Hu, L.; Xu, C. Recent advances in the design of polymeric microneedles for transdermal drug delivery and biosensing. *Lab Chip* **2017**, *17*, 1373–1387. [CrossRef] [PubMed]
146. Liu, T.; Chen, M.; Fu, J.; Sun, Y.; Lu, C.; Quan, G.; Pan, X.; Wu, C. Recent advances in microneedles-mediated transdermal delivery of protein and peptide drugs. *Acta Pharm. Sin. B* **2021**, *11*, 2326–2343. [CrossRef]
147. Singh, P.; Carrier, A.; Chen, Y.; Lin, S.; Wang, J.; Cui, S.; Zhang, X. Polymeric microneedles for controlled transdermal drug delivery. *J. Control. Release* **2019**, *315*, 97–113. [CrossRef] [PubMed]
148. Cheng, H.; Liu, M.; Du, X.; Xu, J.; Zhai, Y.; Ji, J.; He, S.; Zhai, G. Recent progress of micro-needle formulations: Fabrication strategies and delivery applications. *J. Drug Deliv. Sci. Tec.* **2019**, *50*, 18–26. [CrossRef]
149. Leone, M.; Monkare, J.; Bouwstra, J.A.; Kersten, G. Dissolving Microneedle Patches for Dermal Vaccination. *Pharm. Res.* **2017**, *34*, 2223–2240. [CrossRef]
150. Fukushima, K.; Ise, A.; Morita, H.; Hasegawa, R.; Ito, Y.; Sugioka, N.; Takada, K. Two-layered dissolving microneedles for percutaneous delivery of peptide/protein drugs in rats. *Pharm. Res.* **2011**, *28*, 7–21. [CrossRef]
151. Chen, C.H.; Shyu, V.B.; Chen, C.T. Dissolving Microneedle Patches for Transdermal Insulin Delivery in Diabetic Mice: Potential for Clinical Applications. *Materials* **2018**, *11*, 1625. [CrossRef] [PubMed]
152. Ling, M.H.; Chen, M.C. Dissolving polymer microneedle patches for rapid and efficient transdermal delivery of insulin to diabetic rats. *Acta Biomater.* **2013**, *9*, 8952–8961. [CrossRef] [PubMed]
153. Lau, S.; Fei, J.; Liu, H.; Chen, W.; Liu, R. Multilayered pyramidal dissolving microneedle patches with flexible pedestals for improving effective drug delivery. *J. Control. Release* **2017**, *265*, 113–119. [CrossRef] [PubMed]
154. Chen, Y.; Yang, Y.; Xian, Y.; Singh, P.; Feng, J.; Cui, S.; Carrier, A.; Oakes, K.; Luan, T.; Zhang, X. Multifunctional Graphene-Oxide-Reinforced Dissolvable Polymeric Microneedles for Transdermal Drug Delivery. *ACS Appl. Mater. Interfaces* **2020**, *12*, 352–360. [CrossRef] [PubMed]
155. Wang, M.Z.; Niu, J.; Ma, H.J.; Dad, H.A.; Shao, H.T.; Yuan, T.J.; Peng, L.H. Transdermal siRNA delivery by pH-switchable micelles with targeting effect suppress skin melanoma progression. *J. Control. Release* **2020**, *322*, 95–107. [CrossRef]
156. Boone, C.E.; Wang, C.; Lopez-Ramirez, M.A.; Beiss, V.; Shukla, S.; Chariou, P.L.; Kupor, D.; Rueda, R.; Wang, J.; Steinmetz, N.F. Active Microneedle Administration of Plant Virus Nanoparticles for Cancer in situ Vaccination Improves Immunotherapeutic Efficacy. *ACS Appl. Nano Mater.* **2020**, *3*, 8037–8051. [CrossRef]
157. Zeng, Y.; Zhou, H.; Ding, J.; Zhou, W. Cell membrane inspired nano-shell enabling long-acting Glucose Oxidase for Melanoma starvation therapy via microneedles-based percutaneous delivery. *Theranostics* **2021**, *11*, 8270–8282. [CrossRef]
158. Hong, X.; Wei, L.; Wu, F.; Wu, Z.; Chen, L.; Liu, Z.; Yuan, W. Dissolving and biodegradable microneedle technologies for transdermal sustained delivery of drug and vaccine. *Drug Des. Dev. Ther.* **2013**, *7*, 945–952. [CrossRef]
159. Chen, M.C.; Ling, M.H.; Lai, K.Y.; Pramudityo, E. Chitosan microneedle patches for sustained transdermal delivery of macro-molecules. *Biomacromolecules* **2012**, *13*, 4022–4031. [CrossRef]
160. Wang, S.; Zhu, M.; Zhao, L.; Kuang, D.; Kundu, S.C.; Lu, S. Insulin-Loaded Silk Fibroin Microneedles as Sustained Release System. *ACS Biomater.Sci. Eng.* **2019**, *5*, 1887–1894. [CrossRef]
161. Jin, J.; Reese, V.; Coler, R.; Carter, D.; Rolandi, M. Chitin microneedles for an easy-to-use tuberculosis skin test. *Adv. Healthc. Mater.* **2014**, *3*, 349–353. [CrossRef] [PubMed]
162. Chen, M.C.; Lai, K.Y.; Ling, M.H.; Lin, C.W. Enhancing immunogenicity of antigens through sustained intradermal delivery using chitosan microneedles with a patch-dissolvable design. *Acta Biomater.* **2018**, *65*, 66–75. [CrossRef] [PubMed]
163. Justin, R.; Chen, B. Multifunctional chitosan-magnetic graphene quantum dot nanocomposites for the release of therapeutics from detachable and non-detachable biodegradable microneedle arrays. *Interface Focus* **2018**, *8*, 20170055. [CrossRef] [PubMed]
164. Justin, R.; Chen, B. Strong and conductive chitosan-reduced graphene oxide nanocomposites for transdermal drug delivery. *J. Mater. Chem. B* **2014**, *2*, 3759–3770. [CrossRef]
165. Justin, R.; Román, S.; Chen, D.; Tao, K.; Geng, X.; Grant, R.T.; MacNeil, S.; Sun, K.; Chen, B. Biodegradable and conductive chitosan–graphene quantum dot nanocomposite microneedles for delivery of both small and large molecular weight therapeutics. *RSC Adv.* **2015**, *5*, 51934–51946. [CrossRef]
166. Vecchione, R.; Coppola, S.; Esposito, E.; Casale, C.; Vespini, V.; Grilli, S.; Ferraro, P.; Netti, P.A. Electro-Drawn Drug-Loaded Biodegradable Polymer Microneedles as a Viable Route to Hypodermic Injection. *Adv. Funct. Mater.* **2014**, *24*, 3515–3523. [CrossRef]
167. Lin, C.; Metters, A.T. Hydrogels in controlled release formulations: Network design and mathematical modeling. *Adv. Drug Deliv. Rev.* **2006**, *58*, 1379–1408. [CrossRef]
168. Chen, X.; Wang, L.; Yu, H.; Li, C.; Feng, J.; Haq, F.; Khan, A.; Khan, R.U. Preparation, properties and challenges of the microneedles-based insulin delivery system. *J. Control. Release* **2018**, *288*, 173–188. [CrossRef]
169. Eltayib, E.; Brady, A.; Caffarelsalvador, E.; Gonzalezvazquez, P.; Alkilani, A.Z.; Mccarthy, H.O.; Mcelnay, J.; Donnelly, R.F. Hydrogel-forming microneedle arrays: Potential for use in minimally-invasive lithium monitoring. *Eur. J. Pharm. Biopharm.* **2016**, *102*, 123–131. [CrossRef]

170. Yin, Z.; Kuang, D.; Wang, S.; Zheng, Z.; Yadavalli, V.K.; Lu, S. Swellable silk fibroin microneedles for transdermal drug delivery. *Int. J. Biol. Macromol.* **2018**, *106*, 48–56. [CrossRef]

171. Hu, X.; Yu, J.; Qian, C.; Lu, Y.; Kahkoska, A.R.; Xie, Z.; Jing, X.; Buse, J.B.; Gu, Z. H2O2-Responsive Vesicles Integrated with Transcutaneous Patches for Glucose-Mediated Insulin Delivery. *ACS Nano* **2017**, *11*, 613–620. [CrossRef] [PubMed]

172. Yu, J.; Wang, J.; Zhang, Y.; Chen, G.; Mao, W.; Ye, Y.; Kahkoska, A.R.; Buse, J.B.; Langer, R.; Gu, Z. Glucose-responsive insulin patch for the regulation of blood glucose in mice and minipigs. *Nat. Biomed. Eng.* **2020**, *4*, 499–506. [CrossRef] [PubMed]

173. Wang, J.; Yu, J.; Zhang, Y.; Zhang, X.; Kahkoska, A.R.; Chen, G.; Wang, Z.; Sun, W.; Cai, L.; Chen, Z.; et al. Charge-switchable polymeric complex for glucose-responsive insulin delivery in mice and pigs. *Sci. Adv.* **2019**, *5*, eaaw4357. [CrossRef] [PubMed]

174. Wang, Z.; Wang, J.; Li, H.; Yu, J.; Chen, G.; Kahkoska, A.R.; Wu, V.; Zeng, Y.; Wen, D.; Miedema, J.R.; et al. Dual self-regulated delivery of insulin and glucagon by a hybrid patch. *Proc. Natl. Acad. Sci. USA* **2020**, *117*, 29512–29517. [CrossRef] [PubMed]

175. Lin, Y.; Hu, W.; Bai, X.; Ju, Y.; Cao, C.; Zou, S.; Tong, Z.; Cen, C.; Jiang, G.; Kong, X. Glucose- and pH-Responsive Supramolecular Polymer Vesicles Based on Host-Guest Interaction for Transcutaneous Delivery of Insulin. *ACS Appl. Bio. Mater.* **2020**, *3*, 6376–6383. [CrossRef] [PubMed]

176. Yang, X.X.; Feng, P.; Cao, J.; Liu, W.; Tang, Y. Composition-Engineered Metal-Organic Framework-Based Microneedles for Glucose-Mediated Transdermal Insulin Delivery. *ACS Appl. Mater. Interfaces* **2020**, *12*, 13613–13621. [CrossRef]

177. Xu, B.; Jiang, G.; Yu, W.; Liu, D.; Zhang, Y.; Zhou, J.; Sun, S.; Liu, Y. H_2O_2-Responsive mesoporous silica nanoparticles integrated with microneedle patches for the glucose-monitored transdermal delivery of insulin. *J. Mater. Chem. B* **2017**, *5*, 8200–8208. [CrossRef]

178. Tong, Z.; Zhou, J.; Zhong, J.; Tang, Q.; Lei, Z.; Luo, H.; Ma, P.; Liu, X. Glucose- and H_2O_2-Responsive Polymeric Vesicles Integrated with Microneedle Patches for Glucose-Sensitive Transcutaneous Delivery of Insulin in Diabetic Rats. *ACS Appl. Mater. Interfaces* **2018**, *10*, 20014–20024. [CrossRef]

179. Yu, J.; Zhang, Y.; Ye, Y.; DiSanto, R.; Sun, W.; Ranson, D.; Ligler, F.S.; Buse, J.B.; Gu, Z. Microneedle-array patches loaded with hypoxia-sensitive vesicles provide fast glucose-responsive insulin delivery. *Proc. Natl. Acad. Sci. USA* **2015**, *112*, 8260–8265. [CrossRef]